Phosphino-Triazole Ligands for Palladium-Catalysed Cross-Coupling

*Yiming Zhao,[a] Huy van Nguyen,[a] Louise Male,[b] Philip Craven,[a] Benjamin R. Buckley[c] and John S. Fossey[a]**

[a] *School of Chemistry, University of Birmingham, Edgbaston, Birmingham, West Midlands, B15 2TT, UK.*

[b] *X-Ray Crystallography Facility, School of Chemistry, University of Birmingham, Edgbaston, Birmingham, West Midlands, B15 2TT, UK.*

[c] *Department of Chemistry, Loughborough University, Loughborough, Leicestershire, LE11 3TU, UK.*

Abstract

Twelve 1,5-disubtituted and fourteen 5-substituted 1,2,3-triazole derivatives bearing diaryl or dialkyl phosphines at the 5-position were synthesised and used as ligands for palladium-catalysed Suzuki-Miyaura cross-coupling reactions. Bulky substrates were tested, and lead-like product formation was demonstrated. The online tool *SambVca 2.0* was used to assess steric parameters of ligands and preliminary buried volume determination using XRD-obtained data in a small number of cases proved to be informative. Two modelling approaches were compared for the determination of the buried volume of ligands where XRD data was not available. An approach with imposed steric restrictions was found to be superior in leading to buried volume determinations that closely correlate with observed reaction conversions. The online tool *LLAMA* was used to determine lead-likeness of potential Suzuki-Miyaura cross-coupling products, from which ten of the most lead-like were successfully synthesised. Thus, confirming these readily accessible triazole-containing phosphines as highly suitable ligands for reaction screening and optimisation in drug discovery campaigns.

Introduction

Click chemistry, as defined by Sharpless and co-workers,[1] has transformed the face, and accessibility to the non-specialist, of molecular linking strategies. Among click approaches, the highly regioselective copper-catalysed, Huisgen cycloaddition reaction to form 1,4-triazoles (Figure 1, **1**) by Meldal and Sharpless,[1d, 2] has grown in popularity and has been employed in increasingly varied applications over the intervening years.[3] The copper-catalysed azide-alkyne cycloaddition (CuAAC) is ubiquitous,[2, 4] and often referred to as '*the* click reaction,' and the product 1,2,3-triazoles, bearing 1,4-substition patterns, with reliable fidelity and yields being synonymous with click chemistry (Figure 1, **1**).[4b, 5] However, the resulting triazoles are not always employed as innocent by-stander linkage motifs. Triazoles of this type have been used as analogues of peptide linkages (Figure 1, **2**),[6] such peptidomimetics are physiologically stable, and their modular synthesis allows access to a broad range of biologically relevant applications.[7] The utility of further synthetic transformations has been probed, particularly in the derivatisation at the 5-position (Figure 1, **3**).[8]

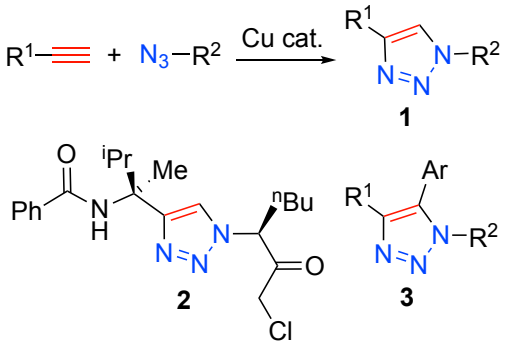

Figure 1. *Upper: Copper-catalysed Azide-Alkyne Cycloaddition (CuAAC); Lower: Examples of 1,2,3-triazole-containing structures.*

Copper-catalysed triazole formation has been exploited in a wide range of scenarios[9] and has been the subject of various mechanistic studies,[10] leading to the proposal of a binuclear transition state involving two copper atoms. 1,2,3-Triazole derivatives have been employed as nitrogen-coordinating ligands,[11] e.g. in *N*,*N*'-,[12] N,S-,[12b] N,Se-[12b] and cyclometallated[13] bidentate coordination complexes. Furthermore tris-triazoles, such as TBTA (Figure 2, **4**) and its analogues, have been used as ligands for reactions including the CuAAC by both Fokin[14] and Zhu[15] and their co-workers, demonstrating exceptional ligand-mediated reaction acceleration.

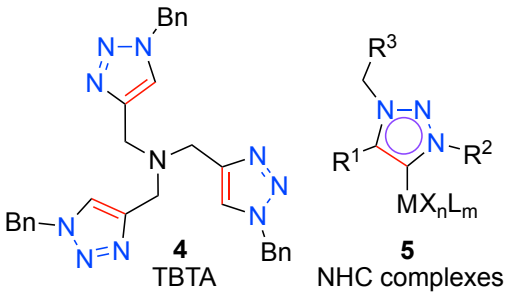

Figure 2. *Examples of triazole-containing or -derived ligands.*

Alkylation of a 1,2,3-triazole derivative, to furnish a 1,3,4-trisubstituted triazolium salt, is the first step in the synthesis of a newer class of *N*-heterocyclic carbene (NHC) reported in 2008 by Albrecht and co-workers,[16] and later extended by Lee and Crowley[17] as ligands for gold and by Grubbs and Bertrand as ligands for ruthenium-mediated catalysis (Figure 2, **5**).[18] The ready access to a range of ligand scaffolds through the CuAAC has led the triazole-NHC platform to continue to gain in popularity.[19] These reports demonstrate the 1,2,3-triazole unit is a legitimate candidate for further exploitation as a key component in ligand design and catalyst development.[20]

Co-authors of this report have investigated triazoles as chemosensors[21] and as products of asymmetric synthesis.[22] Furthermore, an interest in boronic acid derivatives as chemosensors,[23] including the use of cross-coupling reactions as a means of *sensing*,[24] means co-authors of this report are familiar with boronic acids and esters.[25] As such, a desire to bring together these streams of research under one umbrella has led to the research reported in this manuscript. Herein,

the development of bulky and highly active triazole-containing phosphine ligands for palladium-catalysed Suzuki-Miyaura cross-coupling reactions (Scheme 1) is explored.

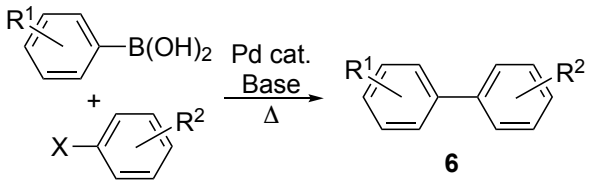

Scheme 1. *Outline of a general palladium-catalysed Suzuki-Miyaura formation of biaryl* ***6****.*

Palladium-catalysed cross-coupling reactions are well studied and offer ready access to an extensive range of (bi)aryl motifs (Scheme 1, **6**).[26] The suite of palladium-catalysed cross-coupling chemistry available for the construction of biologically relevant products has transformed the field of medicinal chemistry, yet cross-coupling between sterically hindered and lead-like building blocks, particularly with aryl chlorides, remains challenging.[27]

Developments in palladium-catalysed chemistry have been heavily influenced by ligand design and optimisation. Among the superior ligands for palladium-catalysed cross-coupling reactions are bulky alkyl phosphines,[28] and bulky *ortho*-substituted aryl-alkyl phosphines,[29] such as S-Phos (Figure 3, **7**)[30] and X-Phos (Figure 3, **8**).[31] Metallocyclic pre-catalysts have been developed which delivered greater stability, more facile manipulation and enhanced reaction outcomes.[32]

Phosphines appended to one or more five-membered, all sp^2, rings have been shown to offer advantages in some cases. The pyrrole-appended phosphines of Beller and co-workers (Figure 3, **9**)[33] have proven to be useful ligands in cross-coupling catalysis that furnishes drug-like products. Furthermore, the bulky, electron-rich, ferrocene-appended phosphines of Richards (Figure 3, **10**),[34] Johannsen (Figure 3, **11**),[35] Fu (Figure 3, **12**)[36] and their respective co-workers provide access to highly active palladium-ligand conjugates for cross-coupling some of the least active substrates.

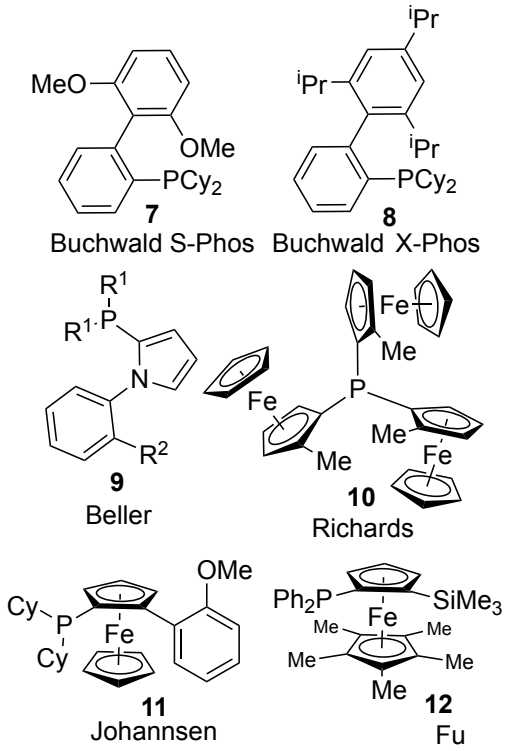

Figure 3. *Representative examples of bulky phosphine ligands including: Upper: S-Phos (**7**) and X-Phos (**8**); Middle left: heteroaromatic phosphine derivative (9); Middle right and lower row: Phosphino-ferrocene derivatives displaying planar chirality.*

1,4-Disubstituted-1,2,3-triazoles have been used in the assembly of phosphorous-containing species that have the potential to be employed as ligands. Ready access to libraries of products using CuAAC reactions has permitted the development of phosphines connected to triazoles with sp^3 linkages to the 1-*N* and 4-*C* positions. Examples include those reported by Dubrovnia, Börner and co-workers (Figure 4, **13**),[37] Gandelman and co-workers who prepared PCP' pincer complexes from bis-phosphinotriazoles (Figure 4, **14**)[38] and Kann and co-workers who used a borane-protected *P*-chiral azide to deliver protected *P*-chiral triazole-containing phosphines (Figure 4, **15**).[39] Since proximal stoichiometric phosphine can arrest the CuAAC through coordinative saturation of sub-stoichiometic copper catalyst or unwanted Staudinger-type reactions between phosphine and azide derivative, alternative approaches are required to deliver *P*-appended triazoles. Zhang and co-workers reported on the use of alkynyl Grignard reagents for the synthesis of a phosphine series where phosphorous is attached directly to a 1,2,3-triazole ring at the 4-position (Figure 4, **16**).[40] As part of an impressive, rigorous and detailed study Balakrishna and co-workers prepared, not only an expected aryl phosphine triazole derivative **17a** (Figure 4), through lithium-halogen exchange and subsequent reaction with diphenylphosphorus chloride on the corresponding bromide under kinetic control, but also the thermodynamically favoured 5-phosphino triazole **18a** (Figure 4) from the same aryl bromide starting material under different conditions.[41] Fukuzawa and co-workers also employed deprotonation of the 5-position of a 1,2,3-triazole to facilitate installation of 5-phosphino functionality in their ferroncenyl bisphosphino ligand synthesis (Figure 4, **19**).[42] Glover *et al.*[43] and Austeri *et al.*[44] also utilised deprotonation of the triazole 5-position to create planar chiral cyclophane-containing

analogues of **18a**. In order to successfully synthesise a bis-5-phosphino-triazole bidentate ligand, Manoury, Virieux and co-workers employed an ethynyl phosphine oxide in their homo-coupled dimer synthesis, which after treatment with trichlorosilane resulted in **20** (Figure 4).[45] A structurally related **5** - **18** hybrid system was also recently reported by Cao *et al.*, who showed the formation of bimetallic complexes of NHC-phosphine mixed systems.[46]

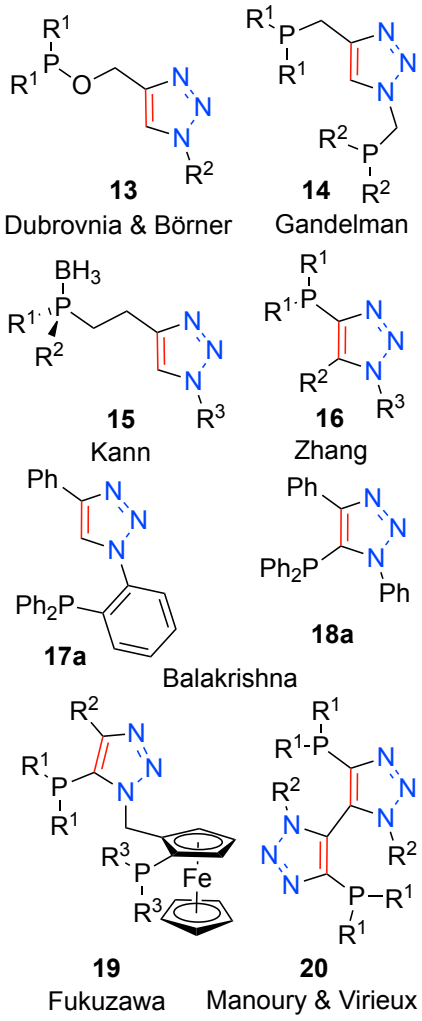

Figure 4. *Phosphorous-containing 1,2,3-triazole derivatives.*

Bulky, or sterically-hindered, phosphorus-containing ligands have also found application outside of the palladium catalysis arena, steric parameters appear to be important in a variety of gold-mediated transformations.[47] Steric and electronic parameters of phosphine ligands have been a subject of study for more than 40 years.[48] More recent contributions have built upon Tolman's concept of *cone angle* as a descriptor of the steric bulk a ligand imparts about a metal, resulting in a parameter known as *buried volume* (%V_{Bur}) coming to the fore.[49] Cavallo and co-workers have developed a free web-based tool for the calculation of %V_{Bur}, named *SambVca*.[50] This parameterisation of ligands, using both spectroscopic measurements and calculated properties (using *principle component analysis* for example), has facilitated exceptional ligand design and optimisation across a range of catalysed reactions.[51]

Whilst a range of ligand-based solutions for cross-coupling reactions exist, a platform to rapidly deliver alternatives and explore chemical space around novel catalyst constructs, such as through CuAAC, offers approaches and complimentary tools to the field. Furthermore, cross-coupling catalysis manifolds that provide access to increasingly three-dimensional products,[52] and those directly delivering products with lead- or drug-like properties[53] without need of protecting group removal or further derivatisation are desired and less-well explored.[27]

Results and Discussion

In order to overcome the general incompatibility of phosphines with the CuAAC reaction, an approach other than direct phosphine incorporation is required. Whilst protection of the phosphine (as a phosphine oxide for example[45]) is possible, the initial approach chosen in this programme was to probe the potential for triazole-mediated directed *ortho*-lithiation or halogen-lithium exchange, and subsequent reaction with diphenyl phosphorous chloride, as possible routes to phosphino-triazoles **17a-c**. Accordingly, 1,4-diphenyl-1,2,3-triazole (**21a**) was selected as a model substrate to test if *ortho*-lithiation could deliver the required intermediate to give the desired product **17a**. As such, **21a** was reacted at -78 °C with *n*-butyllithium, followed by addition of the phosphorous chloride reagent, before being allowed to warm to room temperature, and being allowed to stir for a period of time. Over numerous attempts only the unanticipated product **18a** was isolated from such reactions, Scheme 2. This indicates that deprotonation of the 5-position of the triazole is facile, resulting in formation of the observed major product. In order to mitigate against the formation of the unanticipated triazole-phosphine **18a**, brominated triazole derivatives **22a-c** were employed under a similar protocol, with varying amounts of *n*-butyllithium. In all cases the same 5-phosphino-triazole product **18a** was obtained, Scheme 2. In the case of **22a** it was possible to isolate small quantities of the desired product **17a**. X-Ray crystal structures of both **17a** and **18a** were determined as shown in Figure 5.

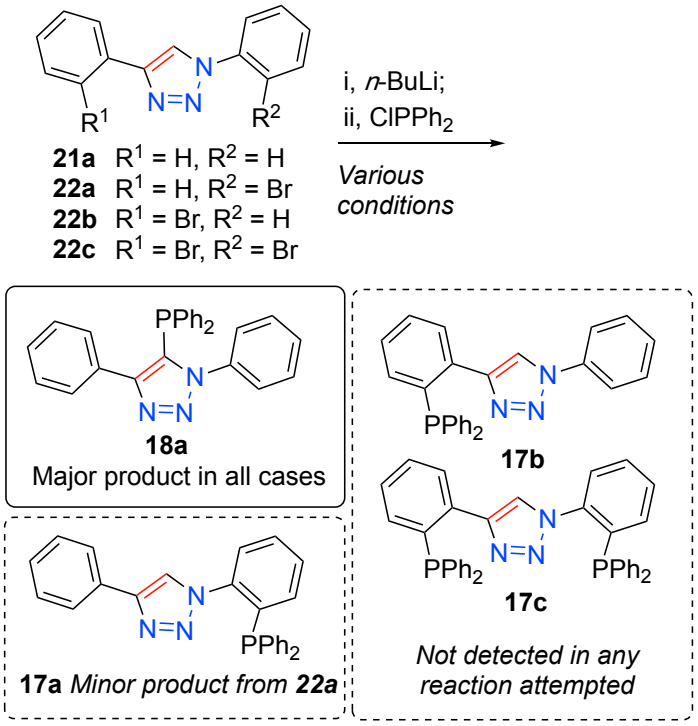

Scheme 2. *Reaction of 1,2,3-triazoles* ***21a-d*** *with n-butyllithium followed by treatment with diphenyl phosphorous chloride led primarily to formation of phosphino-triazole* ***18a****.*

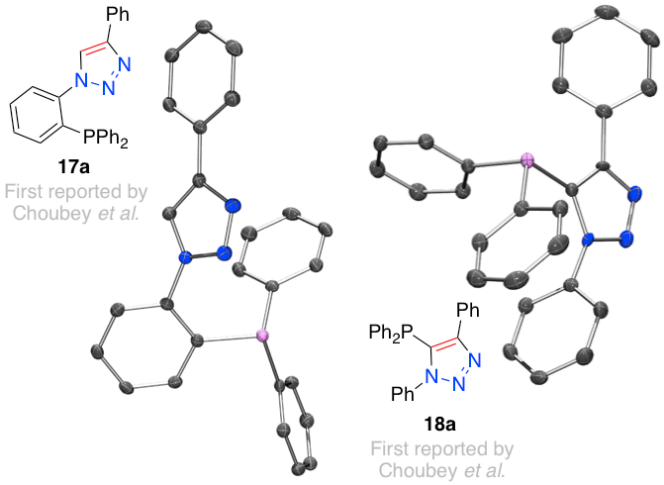

Figure 5. *Representation of the crystal structures of isomeric* ***17a*** *(left) and* ***18a*** *(right), ellipsoids drawn at the 50% probability level (Ortep3 for Windows and PovRay). For* ***17a*** *the structure contains two crystallographically-independent molecules with only one shown for clarity. For* ***18a*** *the phenyl-appended 1-nitrogen and 4-carbon atoms of the triazole unit are disordered such that the triazole ring occupies two opposing orientations, related by a 180° rotation of the triazole ring about the phosphorous-triazole bond. The refined percentage occupancy ratio of the two positions are 59.7 (15) : 40.3 (15), one arbitrary molecule depicted and hydrogen atoms removed for clarity.*

In fact these observations should not have been at all unanticipated.[41, 43] The aforementioned report of Balakrishna and co-workers had previously probed, in more detail than us, the reaction of **17a** under analogous conditions,[41] and determined a 'kinetic' and 'thermodynamic' relationship between lithium-halogen exchange alone, *versus* lithium-

halogen exchange followed by lithium (triazole-) proton exchange leading to products **17a** and **18a** respectively, Scheme 3.

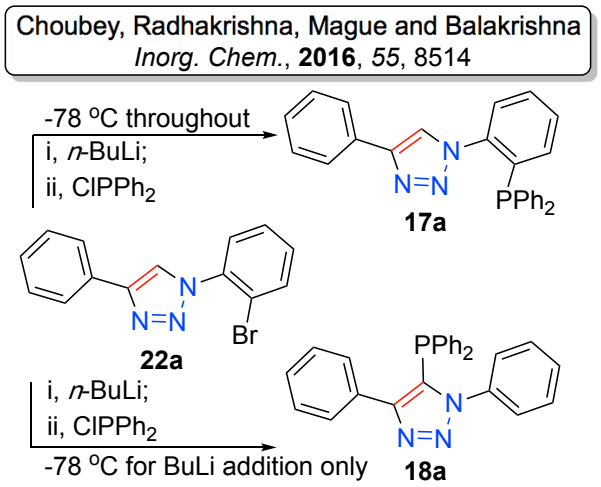

Scheme 3. *Previously reported kinetic (upper) and thermodynamic (lower) lithiation and subsequent phosphorous addition to brominated triazole* ***22a*** *affording P-aryl and P-triazole derivatives respectively.*

Attempts to block the triazole 5-H position, using the deuterium masking approach deployed by Richards and co-workers in the preparation of ferrocene derivatives,[54] did not dramatically modify reaction outcomes in our hands. Variously deuterated products were always obtained from attempted lithiation-mediated access to products under routine conditions.

Since the scope of **18a**-like ligands had not been investigated beyond the three triazole backbones reported by Glover *et al.*[43] and Choubey *et al.*,[41] we chose to focus attention on triazole 5-H lithiation to deliver a range of potential ligands for cross-coupling catalysis. To this end, alkynes **23a** and **23b** reacted smoothly with azides **24a-f** to furnish 1,5-disubstituted 1,2,3-triazoles **21a-i** in acceptable to good yields, Scheme 4.

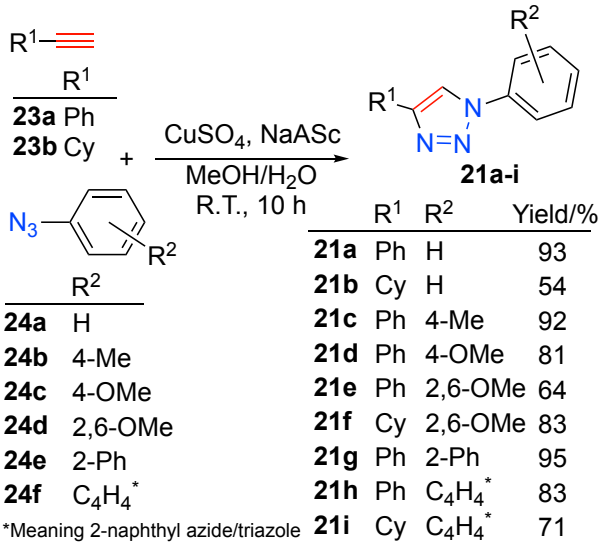

Scheme 4. *CuAAC reaction to form 1,4-disubstituted 1,2,3-triazole derivatives* ***21a-i****.*

Applying the aforementioned triazole lithiation and subsequent quench with dicyclohexyl-, di-*iso*-propyl- or diphenyl-phosphorous chloride reagent protocol to the isolated **21a-i** triazole set, with the express expectation of generating 5-phosphino triazole derivatives, delivered the twelve targeted phosphino-triazoles **18a-l** in acceptable to good yields (Scheme 5).

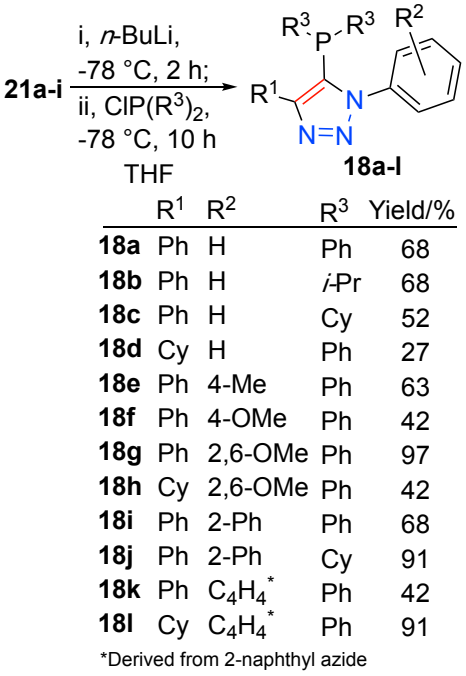

Scheme 5. *Deprotonation and subsequent reaction with phosphorous chloride reagent protocol for delivery of* ***18a-l****.*

In order to benchmark the catalytic capability of ligands in this report, the palladium-catalysed Suzuki-Miyaura reaction of 2-bromo-*m*-xylene (**25**) and *ortho*-tolylboronic acid (**26**) under standard conditions (1 mol% palladium, 2

mol% ligand, three equivalents of base, 10 hours, toluene, 90 °C, see E.S.I) was compared. The catalysed formation of compound **27** represents a challenging but achievable cross-coupling; whilst an arylbromide is employed in the reaction, the product (a triply *ortho*-substituted biaryl) is sterically congested about the formed bond. Diphenyl aryl phosphine **17a** and 5-phosphino triazoles **18a-l** were employed as ligands in the benchmark reaction (Table 1). The use of **17a** as ligand (Table 1, entry 1) resulted in 29% conversion to product **27**. The 5-phosphino isomer of **17a**, **18a**, also gave less than 50% conversion to desired product **27** in the same reaction (Table 1, entry 2). As may be expected, switching the diphenylphosphine part of **18a** to dialkylphosphine groups di-*iso*-propyl (**18b**) and di-cyclohexyl (**18c**) improved the reaction outcomes, resulting in 62 and 75% conversion respectively (Table 1, entries 3 and 4). Changing the alkyne-derived part of the triazole from phenyl (**18a**) to cyclohexyl (**18d**) gave a marked improvement delivering product **27** in 86% conversion (Table 1, entry 2 *versus* 5).

Table 1. *Ligand screening: 1,4-Disubstituted 1,2,3-triazole-containing phosphine ligand mediate, palladium-catalysed, formation of* ***27****.*

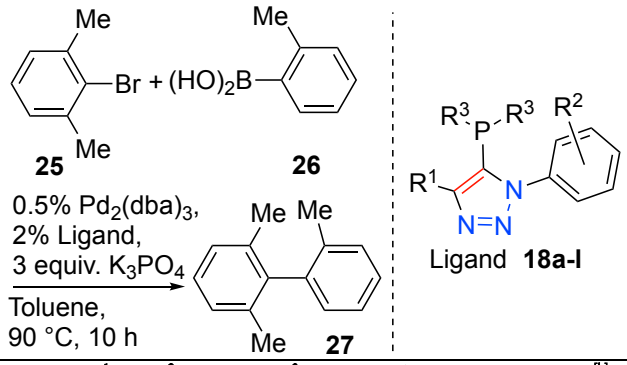

Entry	R^1	R^2	R^3	Ligand	Conversion [%] [b]
1	-	-	-	**17a**	29
2	Ph	H	Ph	**18a**	47
3	Ph	H	*i*-Pr	**18b**	62
4	Ph	H	Cy	**18c**	75
5	Cy	H	Ph	**18d**	86
6	Ph	4-Me	Ph	**18e**	69
7	Ph	4-OMe	Ph	**18f**	83
8	Ph	2,6-OMe	Ph	**18g**	92
9	Cy	2,6-OMe	Ph	**18h**	90
10	Ph	2-Ph	Ph	**18i**	84
11	Ph	2-Ph	Cy	**18j**	92
12	Ph	2-Napth[c]	Ph	**18k**	91
13	Cy	2-Napth[c]	Ph	**18l**	99

[a] Reaction conditions: 2-Bromo-*m*-xylene (0.4 mmol), *o*-tolylboronic acid (0.6 mmol), potassium phosphate (1.2 mmol), $Pd_2(dba)_3$ (0.5 mol%), ligand (2 mol%), toluene (3 mL), 10 h, 90 °C. [b] Conversion determined by inspection of the corresponding ^{1}H NMR spectrums of crude reaction isolates.[55] [e] Meaning derived from naphthyl azide.

Whilst good results were obtained in the Suzuki-Miyaura cross-coupling reactions with **18**-derived catalysts the more effective ligands (generally larger) suffered somewhat from poor solubility. Thus, ligand modifications that retained activity but allowed for more ready synthesis and manipulation at larger scale were sought. From briefly surveying the results in Table 1 it was concluded that changes in the R^1 (alkyne-derived) part (e.g. entry 8 *versus* 9) were less influential on the reaction outcome than changes in the R^2 (azide-derived) part (e.g. entry 5 *versus* 13). Reasoning that *smaller* ligands may benefit from enhanced solubility and tractability, a strategy to retain the *N*-substituents (azide-derived parts), whilst minimising the alkyne-derived parts was chosen for further elaboration. Gevorgyan and co-workers have

already reported that 1,5-disubstituted 1,2,3-triazoles may be accessed by selective reaction at the 5-position of 1-substituted triazoles (Figure 6), and this coupled with the synthetic strategies reported by Oki *et al.*[42] for chiral bisphosphine synthesis led to the conclusion that 1-substitutued triazoles may be readily converted to a library of 1-substituted, 5-phosphino 1,2,3-triazoles

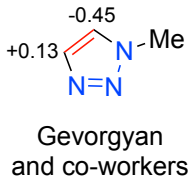

Figure 6. *Electrostatic potential charges as determined by Gevorgyan and co-workers,[8a] indicates rationale for selective C-5 deprotonation.*

Following the optimised protocol of Oki *et al.*,[42] deployed in the synthesis of more complex constructs, a range of 1-substituted triazoles were synthesised. Specifically, trimethylsilylacetylene (**23c**) and aryl azides (**24a-i**) were exposed to CuAAC reaction conditions (Scheme 6), that led to effective triazole formation and desilylation in one pot. Acceptable to good yields of 1-substituted triazoles **28a-i** were isolated after 24-hour, room-temperature, reactions.

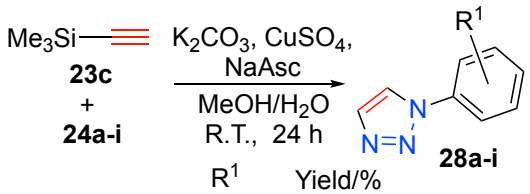

	R^1	Yield/%
28a	H	71
28b	4-Me	84
28c	4-OMe	85
28d	2,6-OMe	64
28e	2-Ph	28
28f	C_4H_4*	40
28g	4-CF_3	72
28h	3,5-OMe	85
28i	2,6-*i*-Pr	40

*Derived from 2-naphthyl azide

Scheme 6. *Trimethylsilylacetylene (**23c**) and aryl azides (**24a-i**) react under desilylative CuAAC reaction conditions to deliver 1-substituted 1,2,3-triazoles (**28a-i**).*

Triazoles **28a-i** reacted smoothly under the deprotonation and phosphorus chloride reagent quench reaction conditions described earlier. Deprotonation at -78 °C, by treatment with *n*-butyllithium, followed by addition of dicyclohexyl-, di-*iso*-propyl-, di-*tert*-butyl- or diphenyl- phosphorous chloride at the same temperature (Scheme 7) resulted in formation of the desired triazole-containing phosphines **29a-n** in acceptable to good yields. The X-ray crystal structure of **29g** was determined (Figure 7); the orientation of the molecule (in the solid state) is such that the lone pair of the phosphine is oriented to the same direction as the 1-aryl substituent of the triazole. In turn, this orientation about a central five-membered ring describes a relatively wide binding pocket for metals with potential for arene-metal interactions alongside primary phosphorous-metal ligation.

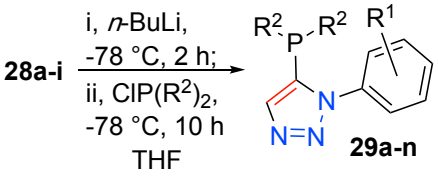

	R^1	R^2	Yield/%
29a	H	Ph	47
29b	H	Cy	73
29c	4-Me	Ph	36
29d	4-OMe	Ph	49
29e	2,6-OMe	Ph	82
29f	2,6-OMe	*i*-Pr	88
29g	2,6-OMe	Cy	73
29h	2,6-OMe	*t*-Bu	72
29i	2-Ph	Ph	27
29j	C_4H_4*	Ph	37
29k	4-CF_3	Ph	68
29l	3,5-OMe	Ph	72
29m	2,6-*i*-Pr	Cy	89
29n	2,6-*i*-Pr	*t*-Bu	88

*Derived from 2-naphthyl azide

Scheme 7. *Deprotonation of 1-aryl 1,2,3-triazole derivatices and subsequent reaction with phosphorous chloride reagent protocol for delivery of* ***29a-n****.*

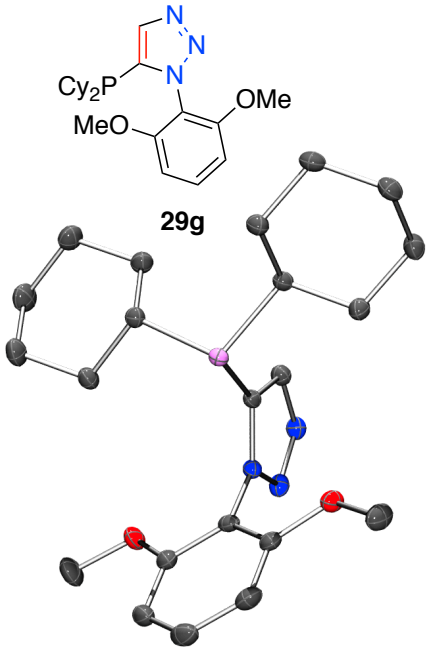

Figure 7. *Representation of the crystal structure of* ***29g****, ellipsoids drawn at the 50% probability level (Ortep3 for Windows and PovRay), hydrogen atoms omitted for clarity.*

Ligands **29a-n** were tested in the aforementioned benchmark Suzuki-Miyaura cross-coupling reaction of **25** with **26** catalysed by a palladium-phosphine complex, to produce biaryl **27** (Table 2, entries 1 to 14). Under the same conditions, commercially sourced ligands, S-Phos (**7**) and X-Phos (**8**) were also used for comparison (Table 2, entries

15 and 16 respectively). Diphenyl-phosphino triazole derived ligands failed to deliver product **27** in good yields, under the conditions employed the best conversion for this ligand class was only 54% (ligand **29c**, Table 2, entry 3). Whereas dialkyl-phosphino triazoles gave universally excellent conversion, equal to the commercially-sourced S- and X-Phos in performance, under these conditions.

Table 2. *Ligand screening: 1-Substituted 1,2,3-triazole-containing phosphine ligand mediated, palladium-catalysed, reaction of arylbromide* ***25*** *in the formation of* ***27****.*

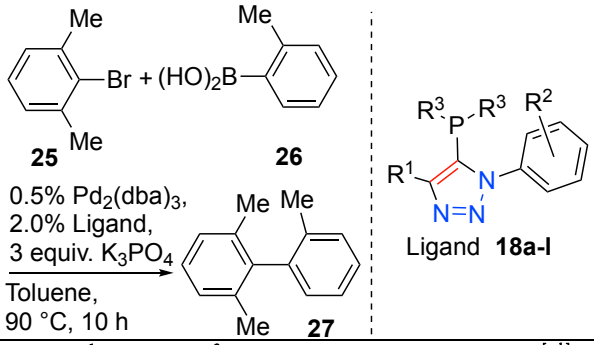

Entry	R^1	R^2	Ligand	Conversion [%] [a, b]
1	H	Ph	**29a**	20
2	H	Cy	**29b**	98
3	4-Me	Ph	**29c**	54
4	4-OMe	Ph	**29d**	28
5	2,6-OMe	Ph	**29e**	90
6	2,6-OMe	*i*-Pr	**29f**	99
7	2,6-OMe	Cy	**29g**	99
8	2,6-OMe	*t*-Bu	**29h**	98
9	2-Ph	Ph	**29i**	82
10	C_4H_4[c]	Ph	**29j**	29
11	4-CF_3	Ph	**29k**	83
12	3,5-OMe	Ph	**29l**	51
13	2,6-*i*-Pr	Cy	**29m**	99
14	2,6-*i*-Pr	*t*-Bu	**29n**	99
15	-	-	S-Phos (**7**)	98
16	-	-	X-Phos (**8**)	99

[a] Reaction conditions: 2-Bromo-*m*-xylene (0.4 mmol), *o*-tolylboronic acid (0.6 mmol), potassium phosphate (1.2 mmol), $Pd_2(dba)_3$ (0.5 mol%), ligand (2.0 mol%), toluene (3 mL), 10 h, 90 °C. [b] Conversion determined by inspection of the corresponding ^{1}H NMR spectrums of crude reaction isolates.[56] [c] Derived from 2-naphthyl azide.

Whilst pleased to have created ligands offering good performance in a benchmark reaction, the reaction itself did not offer enough diversity of outcomes to evaluate dialkyl-phosphino ligand performances against each other nor against the readily available commercial ligands **7** and **8**. Next, a more sterically-demanding test-reaction was chosen to evaluate the ligands further. The formation of biaryl C-C bonds where the formed bond is flanked by four *ortho*-substituents presents a particularly challenging yet attractive transformation, not least due to the apparent three-dimensional nature of the cross-coupled products.[52] The reaction of bromide **30** with boronic acid **31** was selected as one such reaction to probe catalyst effectiveness (Table 3). Conversion to product **32** may be monitored by gas chromatographic analysis, facilitating ready comparison of reactions performed in parallel. Having given quantitative conversions to product **27** (Table 2, entries 7, 8, 13 and 14), and being both relatively easy to synthesise and available in sufficient quantities, ligands **29g**, **29h**, **29m** and **29n** were selected for further investigation. These ligands are triazole-analogues of the

leading phenylene ligands **7** and **8**, thus in order to probe any specific advantages of triazole-core ligands they were compared directly against S-Phos and X-Phos phenylene ligands (for retained and compared ligands see Figure 8).

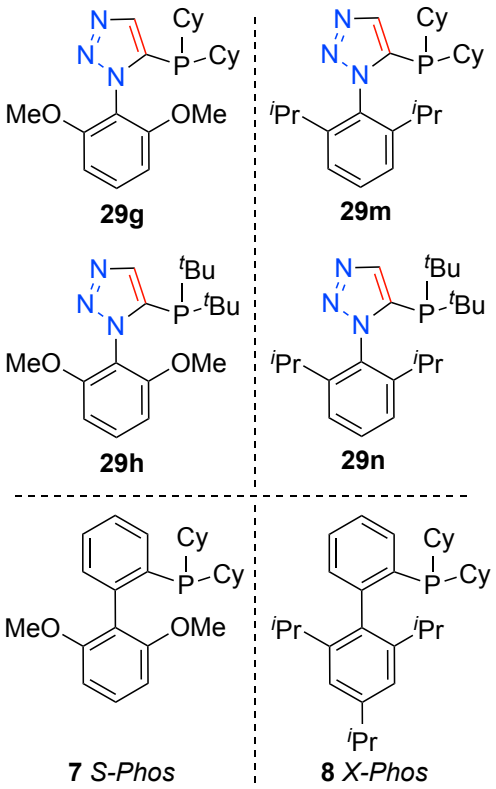

Figure 8. *Ligands compared in Table 3 and Table 4.*

Table 3. *Ligand screening: 1-Substituted 1,2,3-triazole-containing phosphine ligand mediated, palladium-catalysed, reaction of arylbromide* ***30*** *in formation of* ***32****.*

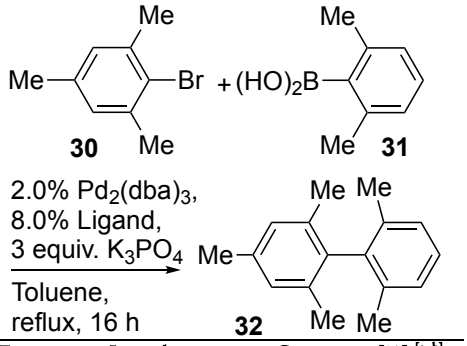

Entry	Ligand	Conversion [%] [a, b]
1	**29g**	99
2	**29g**[c]	84
3	**29h**	47
4	**29m**	60
5	**29n**	13
6	S-Phos (**7**)	87
7	X-Phos (**8**)	50

[a] Reaction conditions: 2-Bromomesitylene (0.5 mmol), 2,6-xylylboronic acid (1.0 mmol), potassium phosphate (2 mmol), $Pd_2(dba)_3$ (2.0 mol%), ligand (8.0 mol%), toluene (3 mL), 18 h, reflux. [b] Determined by GC analysis with *n*-dodecane as internal standard. [c] $Pd_2(dba)_3$ (0.5 mol%), ligand (2 mol%).

In order to ensure good reaction conversions, the catalyst loading, temperature and reaction time were all increased in comparison to the earlier Suzuki-Miyaura reactions. The standard conditions employed in the comparisons of Table 3 (entries 1 and 3 to 7) were 4 mol% palladium, 8 mol% ligand, in toluene at reflux for 16 hours. Under these conditions, cyclohexyl-substituted triazole-containing ligands **29g** and **29m** gave higher conversions to **32** than their *tert*-butyl-substituted analogues **29h** and **29n** (Table 3, entries 1 and 4 (99% and 60%) *versus* entries 3 and 5 (47% and 13%) respectively). In this comparison, the use of S-Phos (**7**) as ligand gave 87% conversion (Table 3, entry 6) and the use of X-Phos (**8**) as ligand gave 50% conversion (Table 3, entry 7) to compound **32** (under these conditions). Since ligand **29g** gave the best conversion (under the conditions employed), catalyst loading was reduced to 1 mol% palladium (in the form of 0.5 mol% $Pd_2(dba)_3$) alongside 2 mol% **29g** as ligand (Table 3, entry 2), and under these conditions, a conversion of 84% to **32** was achieved.

To further probe the utility of 1-aryl 5-phosphino 1,2,3-triazoles as ligands in Suzuki-Miyaura catalysis the synthesis of compound **27** from aryl chloride **37** and boronic acid **26** was investigated (shown in Table 4) deploying the same ligand set as in Table 3. The reaction conditions mirrored those used earlier for cross-coupling with bromide analogue **25** in Table 2 but in order to ensure good reaction conversions the reaction temperature was increased slightly (toluene at reflux).

Table 4. *Ligand screening: 1-Substituted 1,2,3-triazole-containing phosphine ligand-mediated, palladium-catalysed, reaction of arylchloride* ***37*** *in the formation of* ***27****.*

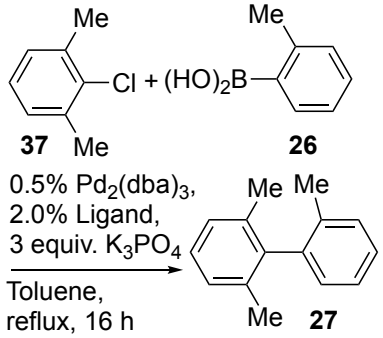

Entry	Ligand	Conversion [%] [a, b]	Isolated yield [%]
1	**29g**	99	93
2	**29g**[c]	99	92
3	**29h**	99	82
4	**29m**	99	92
5	**29n**	70	-
6	S-Phos (**7**)	33	25
7	X-Phos (**8**)	99	90

[a] Reaction conditions: 2-Chloro-*m*-xylene (1.0 mmol), *o*-tolyboronic acid (1.5 mmol), potassium phosphate (3.0 mmol), $Pd_2(dba)_3$ (0.5 mol%), ligand (2.0 mol%), toluene (3 mL), 10 h, 90 °C. [b] Determined by GC analysis with *n*-dodecane as internal standard. [c] $Pd_2(dba)_3$ (0.25 mol%), ligand (1.0 mol%).

Under the reaction conditions employed (Table 4) catalysts derived from triazole-containing ligands **29g**, **29h** and **29m** delivered compound **27** in quantitative yield (Table 4, entries 1, 3 and 4 respectively). Using **29g** as ligand at a lower catalyst loading of 0.5 mol% of palladium proportionally, quantitative conversion to **27** (isolated yield 92%) was achieved. In this comparison, the use of S-Phos (**7**) as ligand gave 33% conversion (Table 4, entry 6) and the use of X-Phos (**8**) as ligand gave quantitative conversion (Table 4, entry 7) to compound **27**.

Next, a demanding palladium-catalysed reaction between 2-chloro-*meta*-xylene (**37**) and 2,4,6-trimethylphenylboronic acid (**38**) leading to product **32** was attempted. Two triazole ligand-based catalyst systems were compared against catalyst systems derived from S-Phos (**7**) and X-Phos (**8**), see Table 5.

Table 5*. Ligand screening: 1-Substituted 1,2,3-triazole-containing phosphine ligand mediate, palladium-catalysed, reaction of arylchloride **37** in formation of **32**.*

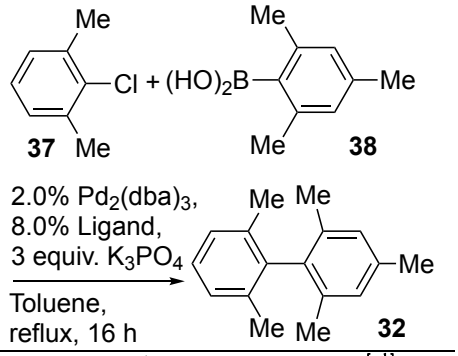

Entry	Ligand	Conversion [%] [a, b]
1	**29g**	49
2	**29m**	37
3	S-Phos (**7**)	55
4	X-Phos (**8**)	5

[a] Reaction conditions: 2-Chloro-*m*-xylene (0.5 mmol), 2,4,6-trimethylphenylboronic acid (1.0 mmol), potassium phosphate (2 mmol), $Pd_2(dba)_3$ (2.0 mol%), ligand (8.0 mol%), toluene (3 mL), 18 h, reflux. [b] Determined by GC analysis with *n*-dodecane as internal standard.

Under the conditions employed the four catalyst systems compared produced only moderate yields. That is not to say that these reactions could not be optimised further, but the side-by-side comparison revealed S-Phos (**7**) to be slightly better than triazole-containing phosphine **29g** (55% *versus* 49% conversion, Table 5 entry 4 *versus* entry 1 respectively). Slightly lower conversions were obtained when **29m** or X-Phos were used as ligands (Table 5 entries 2 and 4 respectively).

One potential problem with Suzuki-Miyaura catalysed reactions, particularly evident when using less reactive aryl chlorides in cross-coupling, is homo-coupling of the boronic acid-containing reaction partner.[57] In order to test our routine reaction protocols and our four selected triazole ligands (**29g**, **29h**, **29m** and **29n**) for their propensity to lead to undesired homo-coupled product, the following reaction was probed. Aryl chloride **33** was reacted with 1.5 equivalents of phenyl boronic acid **34**. Catalyst loading was 2 mol% palladium and 4 mol% ligand. The reactions were conducted in toluene at 90 °C with three equivalents of potassium phosphate as base, see Scheme 8. Set up like this, we can judge a reaction to be successful, i.e. not suffering from an adventitious homo-coupling side reaction leading

to product compromisation, if conversion of aryl chloride **33** is high (near 100%) and the amount of formed by-product **36** is low. Choosing 1.5 equivalents of boronic acid gives chance for the formation of **36** thus evidencing the cross- *versus* homo- coupling potential of the ligands in the chosen Suzuki-Miyaura reaction, under the conditions described.

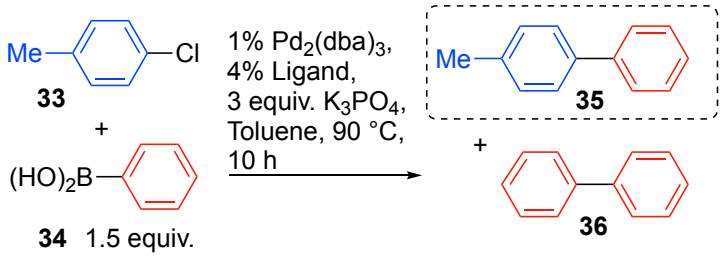

Ligand	Cross-coupled	Homo-coupled
	Conversion **33** [%]	Percent **36** [mol/mol]
29g	96	10%
29h	99	10%
29m	94	12%
29n	99	6%

Scheme 8. *Percentage homo-coupled product **36** under described reaction conditions using 50% excess boronic acid **34**.*

All four of the tested ligands (Scheme 8, **29g**, **29h**, **29m** and **29n**) gave good conversion to product **35** (ligands **29h** and **29n** leading to complete consumption of stating aryl chloride **33**). In this case the apparently *most bulky* ligand **29n** performed best giving just 6% (mol/mol) homo-coupled product (**36**), the other three ligands gave rise to only slightly elevated amounts of homo-coupled side-product (10-12% (mol/mol)). Thus, demonstrating that under the conditions employed, reaction protocols used throughout this study do not suffer appreciably from loss of halide-containing starting materials through unwanted homo-coupling.

Lead-Like Compounds

Whilst the results discussed thus far have exemplified the effectiveness of ligands **29g** and **29m** to catalyse sterically-demanding cross-coupling reactions, the ability to catalyse the cross-coupling of functionalities relevant to medicinal chemistry, to give lead-like and drug-like products remains a critical need in the agrochemical and pharmaceutical sectors.[27] To this end a range of bis-aromatic products, containing motifs of the type that are commonly encountered in medicinal chemistry,[58] were identified and their synthesis embarked upon. The products of virtual Suzuki-Miyaura cross-couplings of 48 aromatic halides (iodides, bromides or chlorides) and 44 aromatic boronic acids (or esters) from: (i) a collection held within the lead research group; (ii) those curated within the *University of Birmingham Scaffold Diversification Resource*;[59] and (iii) drawn from a boronic acid collection *via* the *GSK Free Building Blocks* resource; were enumerated and analysed by the online resource LLAMA (Figure 9).[53]

The open-access LLAMA web tool allows the user to conduct virtual reactions and analyse the virtual product library for molecular properties such as molecular weight, AlogP and 3D-character. Figure 9 left shows the full virtual library of 1661 compounds created from the virtual Suzuki-Miyaura cross-coupling of the boronic acids and aryl halides described above. It shows that, whilst the majority of these virtual products fall within Lipinkski space (Mw <500, AlogP <5), only ~20% lie within lead-like space, as defined by Churcher *et al.* (200 < Mw < 350, AlogP <3). This fact is illustrated by the lead-likeness penalty scores of these compounds, which have an average of 3.47. This penalty scoring system was developed by the creators of LLAMA to visualise how far away from ideal lead-likeness a compound may be, and incorporates all determined molecular properties into one score. Figure 9 right shows the PMI analysis of the same 1661 virtual compounds in the library of virtual Suzuki-Miyaura cross-coupled products. A PMI plot describes the 3D shape of the lowest energy conformation of a compound on a triangular plot. The upper left corner represents rod-like compounds, the bottom corner represents disc-like compounds and the upper right corner represents spherical compounds. This analysis shows that the majority of the virtual library resides close to the rod-disc axis, representing flat compounds.

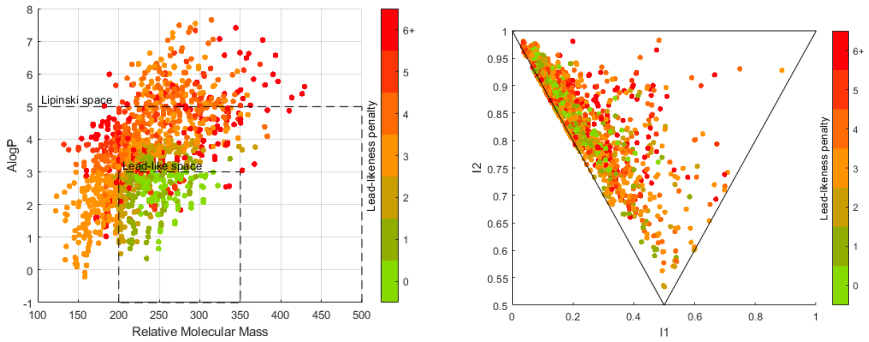

Figure 9. *Virtual Suzuki-Miyaura catalysis products generated and analysed in the LLAMA web tool. Left: AlogP* versus *molecular mass, Lipinski and lead-like space indicated; Right: PMI plot, rod, disc, sphere axis (see supplementary material for tables).*

From the 1661 virtual compounds constructed within the LLAMA tool, 14 possible products that accessed preferable lead-like chemical space and were selected for testing **29g**-mediated Suzuki-Miyaura cross-coupling reactions, Scheme 9. In this case, the screening conditions involved microwave heating in a sealed-tube at 100 °C in acetonitrile for just one hour. The possible products include challenging heteroatom-containing and/or *ortho* substituents, representing both a set of possible products displaying favourable characteristics for drug discovery and a robust challenge for road-testing our best new ligand **29g**.

Pleasingly, most of the reactions attempted gave greater than 50% isolated yield of these challenging cross-coupled products (**41a-j**), however 2-bromo-1-methyl-1*H*-imidazole **39g** and (3,5-dimethylisoxazol-4-yl)boronic acid **40g** failed to deliver detectable amounts of desired cross-coupled products in four test scenarios under the conditions employed.

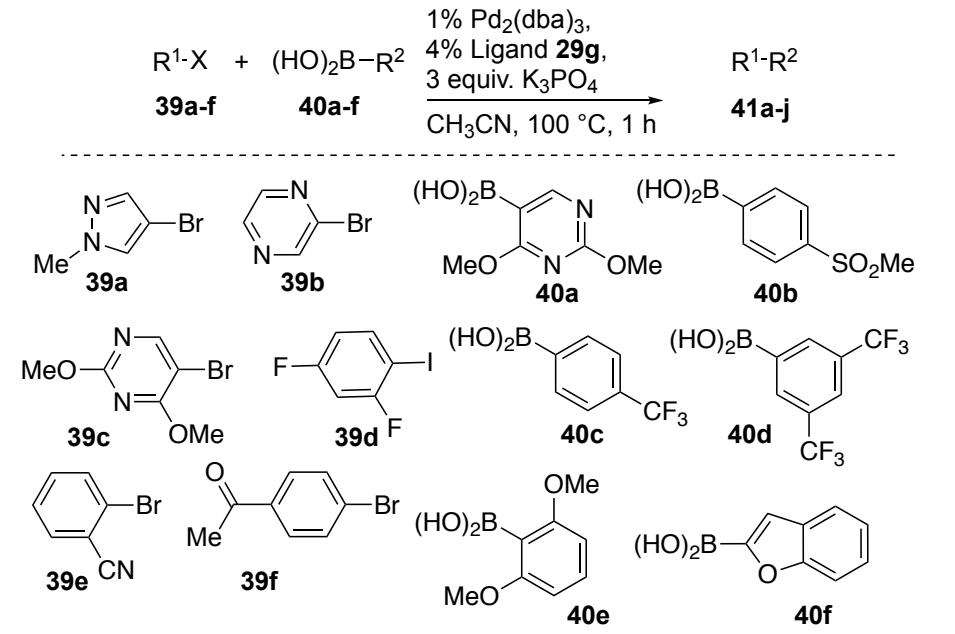
R1-X + (HO)2B–R2
39a-f 40a-f
1% Pd2(dba)3,
4% Ligand 29g,
3 equiv. K3PO4
CH3CN, 100 °C, 1 h
R1-R2
41a-j
39a
39b
40a
40b
39c
39d
40c
40d
39e
39f
40e
40f

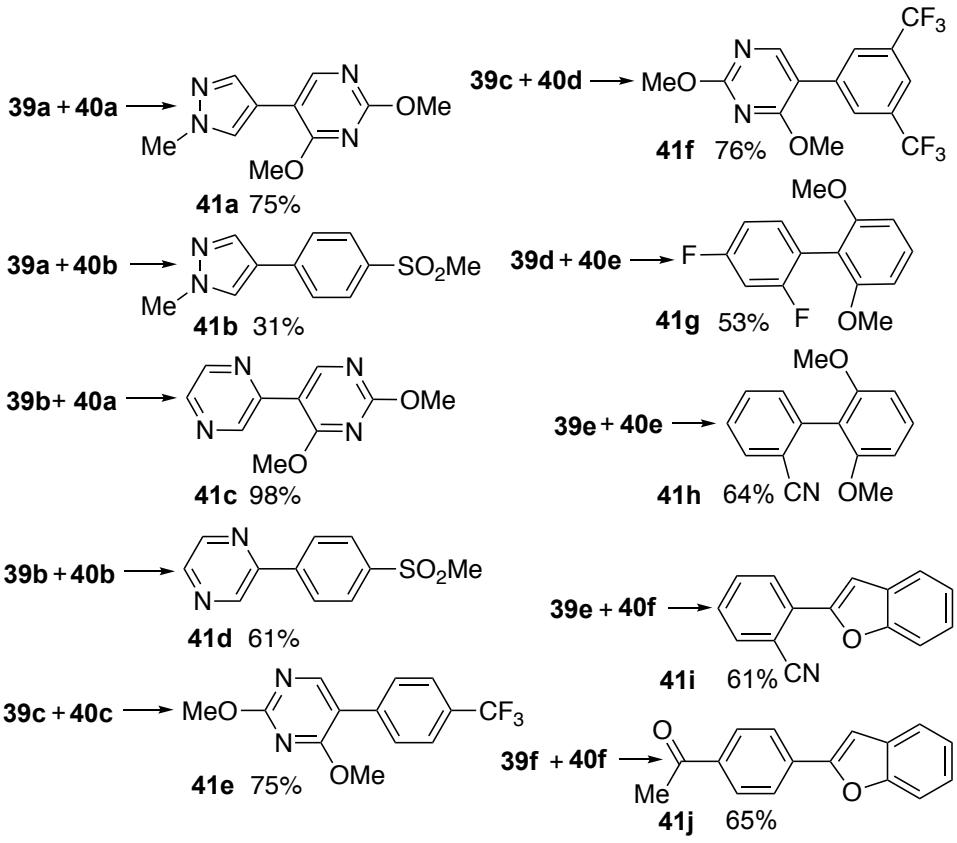
39a + 40a
41a 75%
39a + 40b
41b 31%
39b + 40a
41c 98%
39b + 40b
41d 61%
39c + 40c
41e 75%
39c + 40d
41f 76%
39d + 40e
41g 53%
39e + 40e
41h 64%
39e + 40f
41i 61%
39f + 40f
41j 65%

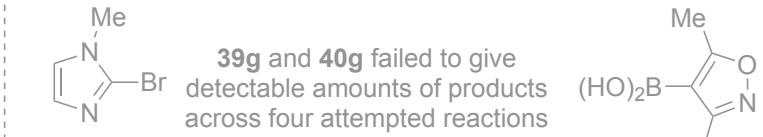
39g
39g and 40g failed to give
detectable amounts of products
across four attempted reactions
40g

***Scheme 9**. The one-hour microwave-heated synthesis of ten lead-like compounds by Suzuki-Miyaura cross-coupling reactions using 2 mol% palladium and 4 mol% ligand **29g**.*

To determine the utility of the products created in this analysis, they were analysed using the LLAMA web tool to determine their suitability as lead-like compounds (Figure 10). Figure 10 (left), shows how products **41a** to **j** explore drug-like space, with all products lying within Lipinski space (Mw <500, AlogP <5) and a significant proportion lying within lead-like space (40% of the synthesised compounds). This illustrates the potential for this catalyst system to access both drug-like and lead-like chemical space. Figure 10 (right), shows a PMI analysis of products **41a** to **j**, this analysis demonstrates a capability of this catalyst system to access non-flat Suzuki-Miyaura cross-coupled products.

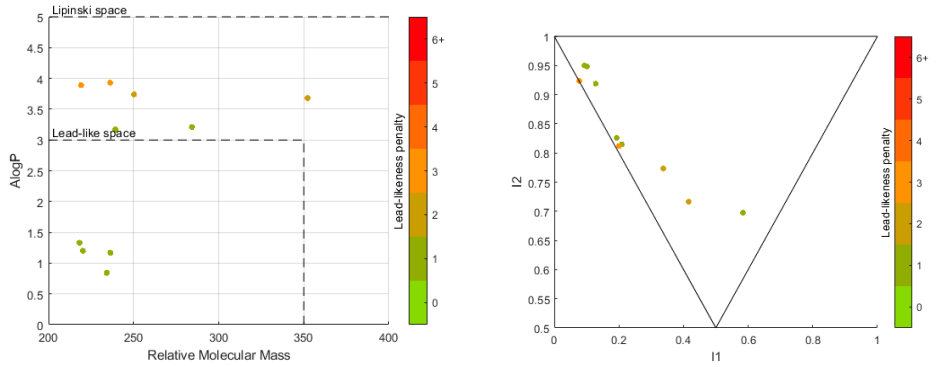

***Figure 10.** Left: Mw vs. AlogP; and Right: PMI analysis of products synthesised in Scheme 9.*

These analyses show that these compounds can be described as high-quality starting points for drug discovery programs. These ten compounds are now under evaluation for biological activity across a range of targets.[60]

Palladium complexes

During the course of this study numerous attempts to grow crystals of palladium-phosphine complexes suitable for single crystal X-ray diffraction were made. Thus far, two attempts to generate X-ray quality crystals of palladium phosphine complexes have been achieved, using ligands **29e** and **29h** with palladium(II) chloride.

The combination of **29e** and *trans*-$Pd(CH_3CN)_2Cl_2$ in dichloromethane at room temperature led to the formation of material that was precipitated by addition of pentane and the residue thus obtained was recrystalised from dichloromethane and hexane. A representation of the single crystal XRD structure of the palladium complex (**42**) thus obtained is depicted in Figure 11. A 2:1 ligand:metal square planar *trans* dichloride palladium(II) complex **42** was identified. Complex **42** may offer insight into the structural features of **29**-series complexes as catalysts. The five-membered 1,5-disubstituted 1,2,3-triazole core presents the triazole 2,6-bismethoxy aryl fragment oriented *towards* the metal with an aryl-centroid…Pd distance of 3.843(2) Å, in this solid-state structure. The triazole phosphine ligand offers a distinct geometric difference to phenylene core ligands (*c.f.* S-Phos and X-Phos, Figure 3), being more akin to

other five-membered ring core ligands (*c.f.* **9**-**10,** Figure 3), generating a slightly wider metal-binding pocket whilst still offering a stabilising shield about the metal centre.

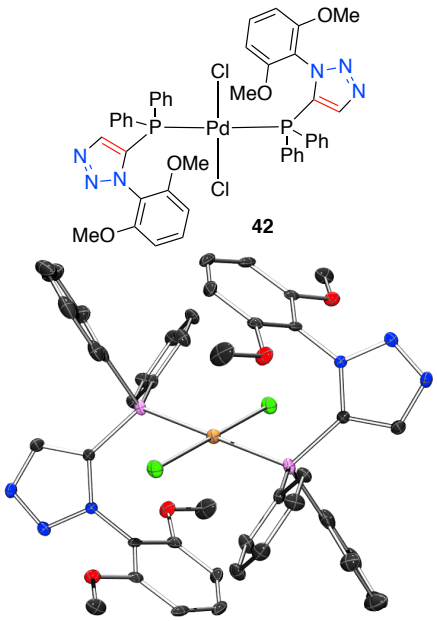

Figure 11. *Representation of the crystal structure of* ***42****, ellipsoids are drawn at the 50% probability level (Ortep3 for Windows and PovRay). The structure contains a palladium complex, which is located on an inversion centre and two molecules of dichloromethane per complex. Only half of the complex and one dichloromethane molecule are unique. Pd…P bond lengths 2.322(9) Å. 2,6-Bismethoxy aryl-centroid…Pd 3.843(2) Å. Symmetry code used to generate equivalent atoms: $1 –x, -y, -z.*

The combination of **29h** and *trans*-Pd(CH_3CN)$_2$$Cl_2$ in dichloromethane at room temperature led to the formation of material that was precepted by addition of pentane and recrystalised from dichloromethane and hexane. A representation of the single crystal XRD structure of the palladium complex (**43**) thus obtained is depicted in Figure 12. To our surprise, the XRD crystal structure shows **29h** functioning as a 3-*N*-coordinating ligand, with two such ligations are present about a *trans*-dichloride palladium(II) metal centre. Since ligand **29h** functions as expected in the aforementioned catalysed reactions it is suggested that a more crystalline and readily formed (kinetic) complex is formed under the crystallisation conditions employed. However, that this stable complex is formed reminds us of another potentially important feature of the triazole-core ligands, namely a rear-side ancillary coordination point. It is conceivable that the ancillary nitrogen may offer some advantages in some catalysed reaction, such as aggregation suppression for example. Suffice it to say, the sterically encumbered phosphine face of ligand **29h**, as evidenced by the isolation of **43**, bodes well for understanding differing catalysis modes of action on steric rationales as well as opportunities for divergence from phenylene core ligands.

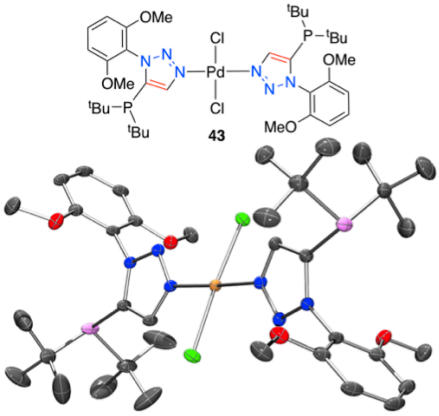

***Figure 12**. Representation of the crystal structure of **43**, ellipsoids are drawn at the 50% probability level (Ortep3 for Windows and PovRay). The structure contains two molecules of dichloromethane per palladium complex (omitted for clarity).*

Describing phosphines

There is a growing body of literature discussing the importance of various parameters including steric effects[51c] of bulky phosphines [29, 61] relating to suitability and efficacy in catalysis (primarily as ligands for metals in metal mediated catalysis).[47a, 51b, 62] Whilst the Tolman cone angle has been an effective descriptor of ligand bulkiness for many years,[48] it has been complimented more recently by Nolan's percentage buried volume parameter (%V_{bur}).[49] The %V_{bur} of ligands can be calculated using the *SambVca* (2.0) free web tool from Cavallo and co-workers;[50, 63] so we set about determining some steric parameters of our phosphines using this tool.

First, the crystal structure of the free ligand **29g** was investigated, as follows: The PDB file corresponding to the XRD crystal structure of ligand **29g** was edited in *Spartan'16 Parallel Suite* (Wavefunction Inc.) by changing the valence of phosphorus to four and adding a palladium atom with a standard bond length of 2.280 Å to generate a metal-coordinated model. The PBD file thus generated was not minimised or edited further (i.e. the atoms of the ligand remained in their crystallographically determined free-ligand position) and uploaded for analysis to the *SambVca* 2.0 web tool for analysis. The added palladium atom was set as the centre and then deleted, a summary of this analysis is shown in Figure 13. A steric map generated from this analysis is shown and a 47.0 %V_{bur} was calculated, using otherwise default *SambVca* settings.

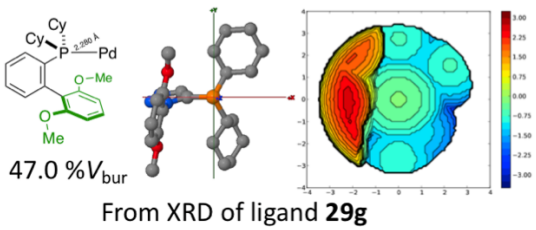

***Figure 13**. Steric map of phosphine-palladium complex: Derived from crystal structure of free ligand **29g** with a P-Pd distance of 2.280 Å applied, resulting in a 47.0 %V_{bur}.*

Following this analysis, the only palladium phosphine complex thus far successfully analysed by single crystal X-ray diffraction studies (**42**) was investigated in a similar manner. Compound **42** is a square planar palladium(II) complex of ligand **29e** and as such does not necessarily represent the catalytically relevant species, the determined %V_{bur} of 36.2% (i. Figure 14) may not be the best comparator across a number of ligand structures so three other forms of the complex were generated and compared. In order to find an appropriate comparison to fairly evaluate relative steric parameters of ligands **29e** and **29g**. The ligand portion of the crystal structure of **42** was edited in *Spartan'16 Parallel Suite* and the Pd-P bond length adjusted to 2.280 Å, and the SambVca-determined %V_{bur} of 36.9% (ii. Figure 14) was essentially the same as that for the slightly longer, crystallographically-determined, Pd-P bond length in the earlier analysis. Since a model to allow for comparison of ligands where crystallographically-determined data is not available was ultimately sought two further analyses were conducted.

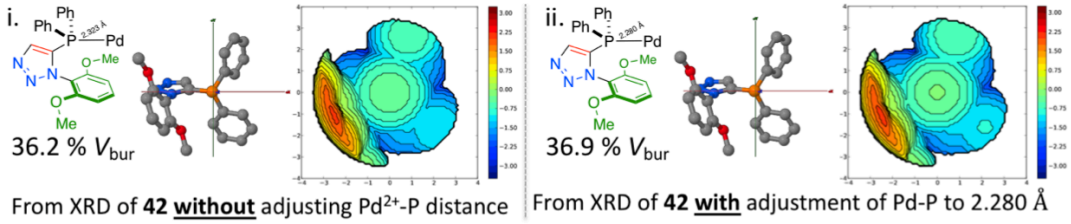

Figure 14. i. *Chemical structure of part of the crystallographically-determined complex* ***42****, with a 2.323(2) Å Pd-P distance (from the crystal structure) used in the calculation of buried volume, 36.2 %*V_{bur}*;* ***ii.*** *Chemical structure of the* bond-length-modified *crystal-structure-informed palladium complex of ligand* ***29e*** *in complex* ***42*** *(a 2.280 Å Pd-P distance was used in the buried volume calculation), 36.9 %*V_{bur}*.*

Sigman and co-workers have previously used phosphine oxides as computational models for structural minimisation proxies of ligand-metal complexes,[51b] so it was reasoned that computational minimisation of *in silico*–generated phosphine oxides may be a sensible starting point to allow for comparison among some of the ligands in this report. Two approaches were compared for optimising and computationally determining the %V_{bur} of ligand **29e** (summarised in Figure 15) using *Spartan'16 Parallel Suite*. In one case a phosphine oxide structure with no geometric restrictions was used (Figure 15, right); in the second case the dihedral geometries of atoms 1 to 6 were restricted presenting the ligand's ancillary aryl group directly and orthogonally aligned to the coordination vector of the phosphine (the P-O bond in this minimisation), as shown in (Figure 15, left). Through comparison of the geometry unrestricted and geometry restricted protocols, with the structurally determined geometry (as shown in Figure 13) a protocol for analysis across the ligands of this report might be reasonably arrived at. In both cases the same minimisation and optimisation cascade was adopted, the structures used for *computationally determined* %V_{bur} calculations were obtained as follows: First, molecular mechanics (MMFF) conformer distribution (1000 max conformers) and subsequent molecular mechanics equilibrium geometries were ranked, and the 20 lowest energy conformers were retained for DFT investigation. The 20 retained conformers' equilibrium geometries were used as starting points for ground state, gas phase equilibrium geometry determination (B3LYP 6-31G*). The lowest energy structure thus obtained was then

edited to replace the oxygen (of the phosphine oxide) with a palladium atom and a standard P-Pd bond length of 2.280 Å was applied (Figure 15, centre).

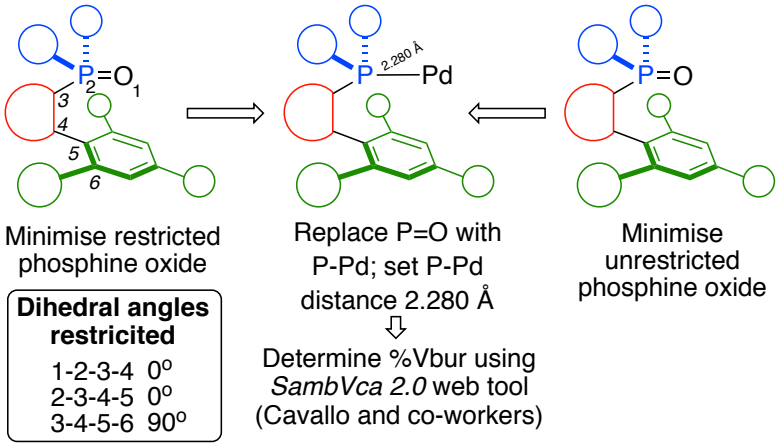

***Figure 15**. The protocol for obtaining structures for comparison of steric parameters* via *an unrestricted (right) and a dihedral angles restricted model (left). In both cases a phosphine oxide model was minimised using* Spartan'16 *and the P=O later replaced with a P-Pd bond of 2.280 Å. The structures thus obtained were then analysed by the* SambVca *2.0 free web tool to determine the* %V_{bur} *and to create a steric map.*

The procedure outlined in Figure 15 was first applied to ligand **29e**, and buried volumes of 44.2 and 47.3% were determined for the restricted and unrestricted geometries, respectively (Figure 16) and compared to the buried volume determined crystallographically. Whilst this protocol gives slightly higher values the restricted geometry model is more closely aligned to the XRD-derived model than the unrestricted one. With this information alone it is difficult to ascertain if any one model provides a superior approach for assessing ligands where solid state data is not available. Furthermore, it should be remembered that the **42**-derived %V_{bur} numbers are from solid state structures and might not offer the best cross-ligand comparison. As such, the most active ligands of our study were examined using both protocols, see below (Figure 17).

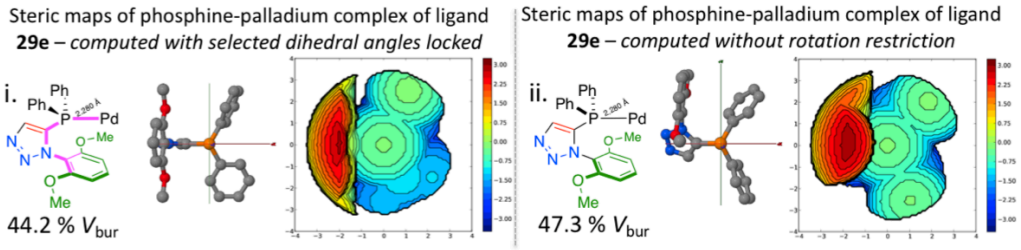

***Figure 16**. **i**. Chemical structure and computationally-determined steric map and buried volume, structures derived* in silico *and calculated with restricted dihedral angles as describe in Figure 15 (left), 44.2 %*V_{bur}*; **ii**. Chemical structure and computationally-determined steric map and buried volume of structures derived* in silico *and calculated without any dihedral restrictions as describe in Figure 15 (right), 47.3 %*V_{bur}.

Computed structures, percentage buried volumes and steric maps of the six ligands of Figure 8, following the protocol outlined in Figure 15 are shown in Figure 17. The left side shows the information relating to restricted dihedral angle restricted complexes and the right side shows the structures obtained without imposing any geometrical restrictions (other than the 2.280 Å P-Pd distances imposed throughout). It is interesting, and confounded our expectations, that

the unrestricted geometry-minimised structures give a higher buried volume than the restricted dihedral angle structures (Figure 17 column a. *versus* column b.). Among the two data treatments there is broad agreement with, and relative similarity to, each other. Whilst the geometry-unrestricted structures of triazole ligands bear a striking resemblance (by rudimentary visual inspection) to any XRD-derived structures, the buried volume determinations of previously reported S- and X-Phos (by the P=O minimisation proxy discussed earlier) complexes more closely match the geometry-restricted models we employed (Table 6, entry 6 and 7).

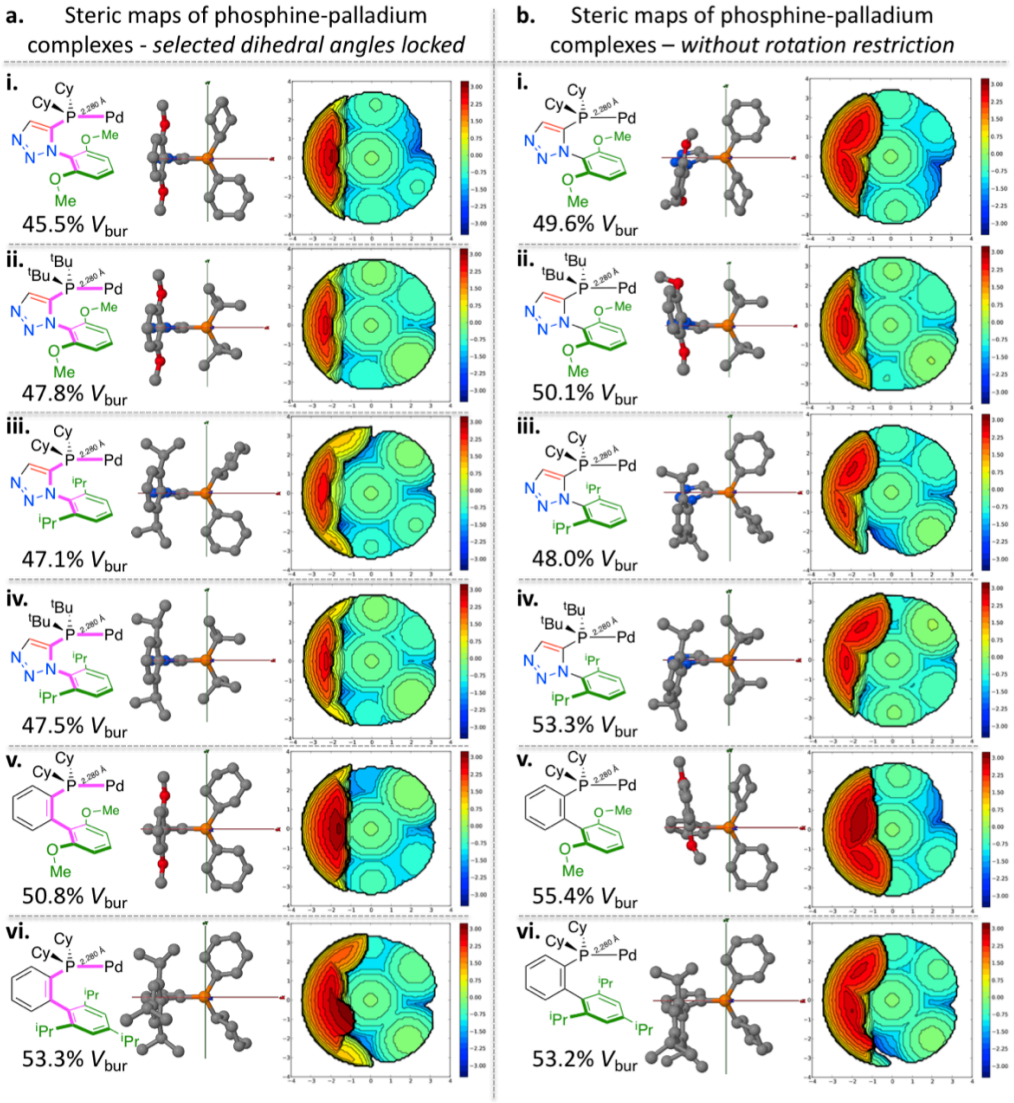

Figure 17. *The* SambVca *2.0 derived* %V_{bur} *and steric maps for the: (a) left side -* ***i. 29g****;* ***ii. 29h****;* ***iii. 29n****;* ***iv. 29m****;* ***v. 7*** *S-Phos;* ***vi. 8*** *X-Phos, derived palladium complexes of structures derived* in silico *and calculated with restricted dihedral angles as describe in Figure 15 (left); (b) rigth side -* ***i. 29g****;* ***ii. 29h****;* ***iii. 29n****;* ***iv. 29m****;* ***v. 7*** *S-Phos;* ***vi. 8*** *X-Phos, derived palladium complexes of structures derived* in silico *and calculated without any dihedral restrictions as describe in Figure 15 (right).*

From the steric maps of Figure 17, it was noted that the space between the dark red *bulky* zone (to the left of the steric maps arising from the ancillary aryl groups of all ligands) protrudes in a manner to give more *space* between the central axis and *red zone*. Since *space* near the coordination site may be crucial in permitting reaction with bulky substrates we

also report the distance between the ancillary aryl group's centroid and the computed metal centre (Table 6) for both the geometry-restricted and unrestricted ligands of Figure 8 are also listed in Table 6 (and contrasted against the data determined for ligand **29e**). In Entry 2 the data arising from analysis of the previously detailed ligand-crystal structure-determined structures of **29g**-complexes are given in parenthesis. Between the restricted and unrestricted models of ligand-complex analysis, the centroid distance correlates more closely with the dihedral angle restricted model of a **29g**-Pd complex.

Table 6. *Calculated (*Spartan *v16 and* SambVca *2.0) steric properties of* ***29e***, ***29g***, ***29h***, ***29m***, ***29n***, *S-Phos* ***7*** *and X-Phos* ***8***.

Entry	Ligand	V_{bur} calc. [%] (restricted)	V_{bur} calc. [%] (unrestricted)	Ar Centroid-Pd distance [Å] (restricted)	Ar Centroid-Pd distance [Å] (unrestricted)
1	**29e**	44.2 (36.2)[a]	47.3	3.363 (3.843(2))[a]	4.176
2	**29g**	45.5 (46.9)[b]	49.6	3.403 (3.457)[b]	3.745
3	**29h**	47.8	50.1	3.558	3.580
4	**29m**	47.1	48.0	3.639	3.901
5	**29n**	47.5	53.3	3.647	3.794
6	**7** *(S-Phos)*	50.8 (49.7)[lit]	55.4	3.127	3.253
7	**8** *(X-Phos)*	53.3 (53.1)[lit]	53.2	3.309	3.481

[a] Measured from the unadjusted XRD structure of **42**; [b] Using free ligand **29g** XRD and applying Pd-P bond length 2.280 Å. [lit] Refers to ligand:metal 1:1 complex P-M distance 2.8 A (M = Au).[49, 64]

It is notable that the P=O ligand minimisation protocol adopted gives good structural parameter agreement between those determined for palladium complexes of ligand **29g** both derived computationally and from a modified XRD structure of free ligand **29g** (Table 6, entry 1). By analysing **29a-n** side-by-side using the same restricted dihedral angle minimisation protocol (up to 10 conformers analysed by DFT methods abbreviating the earlier minimisation cascade for newly analysed ligands) and plotting the computed %V_{bur} values against conversion to **27** (data from Table 2), as shown in Figure 18, it can be seen that a strong bulkiness *versus* conversion trend exists. Essentially any %V_{bur} value above 46% leads to quantitative conversion to products, under the prescribed conditions.

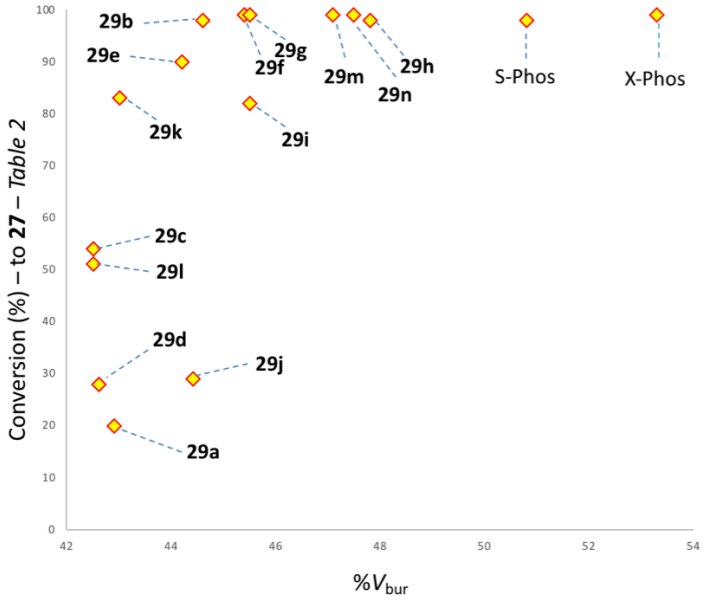

Figure 18*. Conversion to* ***27*** *(see Table 2)* versus *computed burried volume (%) as determined by the protocol discussed in Figure 15.*

Further analysis of the data obtained for conversion in reactions catalysed by **29**-ligands is only against smaller datasets and significant correlations of variances in conversions do not lead to any meaningfully comparable correlations. However, further study of cross-couplings of very bulky aryl chlorides may be warranted in the future since an intriguing balance between bulk and centroid distance is suggested (see ESI) but across only four data points surveyed to-date it may be too early to draw conclusion yet.[65]

Conclusions

Two series of 1,2,3-triazole-containing 5-phosphino ligands were synthesised and tested as ligands in palladium catalysed cross-coupling Suzuki-Miyaura reactions of bulky and heteroatom-containing substrates. The structural parameters of the 4-H triazole series (**29**) were determined by a restricted dihedral angle, phosphine oxide surrogate, model and a strong dependence upon bulkiness and catalytic activity were noted. Furthermore, a link to the space between the metal and the ancillary aryl group in the computed complexes was noted, suggesting bulkiness of ligand and space around the metal may both be implicated in delineating trends in cross-coupling of the most bulky and challenging substrates. Notably, triazole-nitrogens' may not be completely innocent in the coordination environment created by these ligands, with a nitrogen coordination complex being characterised by XRD in one case. The ligands synthesised were benchmarked against commercially available ligands (X- and S-Phos) and in some cases the best triazole ligands match or outperformed them under the employed conditions, in like-for-like tests in triplicate. The phosphine ligands reported and characterised in this report represent easy to modify catalytic scaffolds that could be use in future library generation efforts and we are looking forward to facilitating access to these compounds and allowing others to include this type of ligand in their own catalyst screening campaigns.

Acknowledgements

JSF, YZ, PC, HvN and LM would like to thank the University of Birmingham for support. JSF acknowledges the CASE consortium for networking opportunities.[66] BRB thanks Loughborough University and Research Councils UK for a RCUK Fellowship. JSF would like to thank the Royal Society for an Industrial Fellowship and the EPSRC for funding (EP/J003220/1). Dr Chi Tsang and Dr Peter Ashton are thanked for helpful discussions about mass spectrometry. Dr Cécile S. Le Duff is thanked for advice on NMR spectroscopy. Helena Dodd is thanked for providing an initial data analysis and presentation app for MatLab. JSF and BRB acknowledge the support of a Wellcome Trust ISSF award within the University of Birmingham. All investigators are grateful for a Royal Society Research Grant (2012/R1) that underpins this project. The *GSK free building block* programme furnished a collection of boronic acids from which **40a** was sourced. The *University of Birmingham Scaffold Diversification Resource* is gratefully acknowledged for providing access to a collection of compounds from which **39a-f** and **40b-f** were sourced.

Author Contributions

All authors contributed to the preparation of the manuscript, specific contributions in addition to this are listed for each co-author in alphabetical order: BRB helped direct aspects of the research, initiated some of the steric parameter analysis and gave input and critical assessment throughout the progress of the project; PC analysed molecular property analysis through use of LLAMA and wrote aspects of the manuscript and ESI pertaining to this aspect; JSF led and co-conceived the project, providing critical assessment of data, day-to-day project management and oversight, directed all aspects throughout, supervised the experimental work and wrote the majority of the manuscript; LM is responsible for collecting, analysing and preparing for publication single crystal XRD data, writing aspects of the main text and ESI and training oversight of YZ in aspects of XRD data collection and analysis; HvN conducted all the experiments of Scheme 9 offered additional advice and wrote aspects of the ESI; YZ Co-conceived aspects of the project, conducted all ligand synthesis and all-bar the Scheme 9 reactions, wrote aspects of the main text, drafted a large proportion of the ESI, offered critical suggestions, under the mentorship of LM conducted some of the XRD data collection and analysis.

References

1. (a) M. G. Finn, H. C. Kolb, V. V. Fokin and K. B. Sharpless, *Progress in Chemistry*, 2008, **20**, 1-4; (b) H. C. Kolb, M. G. Finn and K. B. Sharpless, *Angew. Chem., Int. Ed.*, 2001, **40**, 2004; (c) W. G. Lewis, L. G. Green, F. Grynszpan, Z. Radic, P. R. Carlier, P. Taylor, M. G. Finn and K. B. Sharpless, *Angew. Chem., Int. Ed.*, 2002, **41**, 1053-1057; (d) V. V. Rostovtsev, L. G. Green, V. V. Fokin and K. B. Sharpless, *Angew. Chem., Int. Ed.*, 2002, **41**, 2596-2599.
2. C. W. Tornøe, C. Christensen and M. Meldal, *J. Org. Chem.*, 2002, **67**, 3057-3064.
3. Based upon citation reports using Thomas Reuters Web of Science TM for the term "click reaction"
4. (a) M. Meldal and C. W. Tornøe, *Chem. Rev.*, 2008, **108**, 2952-3015; (b) J. E. Moses and A. D. Moorhouse, *Chem. Soc. Rev.*, 2007, **36**, 1249-1262; (c) P. Thirumurugan, D. Matosiuk and K. Jozwiak, *Chem. Rev.*, 2013, **113**, 4905-4979.
5. (a) F. Amblard, J. H. Cho and R. F. Schinazi, *Chem. Rev.*, 2009, **109**, 4207-4220; (b) A. H. El-Sagheer and T. Brown, *Chem. Soc. Rev.*, 2010, **39**, 1388-1405; (c) R. K. Iha, K. L. Wooley, A. M. Nyström, D. J. Burke, M. J. Kade and C. J. Hawker, *Chem. Rev.*, 2009, **109**, 5620-5686; (d) B. Schulze and U. S. Schubert, *Chem. Soc. Rev.*, 2014, **43**, 2522-2571; (e) G. C. Tron, T. Pirali, R. A. Billington, P. L. Canonico, G. Sorba and A. A. Genazzani, *Med. Res. Rev.*, 2008, **28**, 278-308; (f) H. C. Kolb, M. G. Finn and K. B. Sharpless, *Angew. Chem. Int. Ed.*, 2001, **40**, 2004-2021.
6. Z. Zhang and E. Fan, *Tetrahedron Lett.*, 2006, **47**, 665-669.
7. (a) A. W. Patterson, W. J. L. Wood, M. Hornsby, S. Lesley, G. Spraggon and J. A. Ellman, *J. Med. Chem.*, 2006, **49**, 6298-6307; (b) W. J. L. Wood, A. W. Patterson, H. Tsuruoka, R. K. Jain and J. A. Ellman, *J. Am. Chem. Soc.*, 2005, **127**, 15521-15527.
8. (a) S. Chuprakov, N. Chernyak, A. S. Dudnik and V. Gevorgyan, *Org. Lett.*, 2007, **9**, 2333-2336; (b) K. D. B. Yamajala, M. Patil and S. Banerjee, *J. Org. Chem.*, 2015, **80**, 3003-3011.
9. J. Winn, A. Pinczewska and S. M. Goldup, *J. Am. Chem. Soc.*, 2013, **135**, 13318-13321.
10. (a) M. Ahlquist and V. V. Fokin, *Organometallics*, 2007, **26**, 4389-4391; (b) B. R. Buckley, S. E. Dann and H. Heaney, *Chem.-Eur. J.*, 2010, **16**, 6278-6284; (c) B. R. Buckley, S. E. Dann, D. P. Harris, H. Heaney and E. C. Stubbs, *Chem. Commun.*, 2010, **46**, 2274-2276; (d) B. T. Worrell, J. A. Malik and V. V. Fokin, *Science*, 2013, **340**, 457-460; (e) A. Makarem, R. Berg, F. Rominger and B. F. Straub, *Angew. Chem., Int. Ed.*, 2015, **54**, 7431-7435.
11. P. I. P. Elliott, in *Organometallic Chemistry: Volume 39*, eds. I. J. S. Fairlamb and J. M. Lynam, The Royal Society of Chemistry, 2014, vol. 39, pp. 1-25.
12. (a) D. Schweinfurth, R. Pattacini, S. Strobel and B. Sarkar, *Dalton Trans.*, 2009, 9291-9297; (b) S. Kumar, F. Saleem and A. K. Singh, *Dalton Trans.*, 2016, **45**, 11445-11458; (c) G. Zhang, Y. Wang, X. Wen, C. Ding and Y. Li, *Chem. Commun.*, 2012, **48**, 2979-2981; (d) S. Hohloch, D. Schweinfurth, M. G. Sommer, F. Weisser, N. Deibel, F. Ehret and B. Sarkar, *Dalton Trans.*, 2014, **43**, 4437-4450; (e) E. P. McCarney, C. S. Hawes, S. Blasco and T. Gunnlaugsson, *Dalton Trans.*, 2016, **45**, 10209-10221; (f) I. Bratsos, D. Urankar, E. Zangrando, P. Genova-Kalou, J. Kosmrlj, E. Alessio and I. Turel, *Dalton Trans.*, 2011, **40**, 5188-5199; (g) B. Chowdhury, S. Khatua, R. Dutta, S. Chakraborty and P. Ghosh, *Inorg. Chem.*, 2014, **53**, 8061-8070.

13. (a) J. M. Fernández-Hernández, C.-H. Yang, J. I. Beltrán, V. Lemaur, F. Polo, R. Fröhlich, J. Cornil and L. De Cola, *J. Am. Chem. Soc.*, 2011, **133**, 10543-10558; (b) K. N. Swanick, S. Ladouceur, E. Zysman-Colman and Z. Ding, *Chem. Commun.*, 2012, **48**, 3179-3181; (c) S. Ladouceur, D. Fortin and E. Zysman-Colman, *Inorg. Chem.*, 2011, **50**, 11514-11526.

14. T. R. Chan, R. Hilgraf, K. B. Sharpless and V. V. Fokin, *Org. Lett.*, 2004, **6**, 2853-2855.

15. H. A. Michaels and L. Zhu, *Chem. Asian J.*, 2011, **6**, 2825-2834.

16. P. Mathew, A. Neels and M. Albrecht, *J. Am. Chem. Soc.*, 2008, **130**, 13534-13535.

17. (a) K. J. Kilpin, U. S. D. Paul, A.-L. Lee and J. D. Crowley, *Chem. Commun.*, 2011, **47**, 328-330; (b) J. D. Crowley, A.-L. Lee and K. J. Kilpin, *Aust J Chem*, 2011, **64**, 1118-1132; (c) J. R. Wright, P. C. Young, N. T. Lucas, A.-L. Lee and J. D. Crowley, *Organometallics*, 2013, **32**, 7065-7076.

18. J. Bouffard, B. K. Keitz, R. Tonner, G. Guisado-Barrios, G. Frenking, R. H. Grubbs and G. Bertrand, *Organometallics*, 2011, **30**, 2617-2627.

19. (a) T. Nakamura, T. Terashima, K. Ogata and S.-i. Fukuzawa, *Org. Lett.*, 2011, **13**, 620-623; (b) M. Flores-Jarillo, D. Mendoza-Espinosa, V. Salazar-Pereda and S. González-Montiel, *Organometallics*, 2017, **36**, 4305-4312; (c) J. Schmid, W. Frey and R. Peters, *Organometallics*, 2017, **36**, 4313-4324; (d) M. A. Kinzhalov, A. S. Legkodukh, T. B. Anisimova, A. S. Novikov, V. V. Suslonov, K. V. Luzyanin and V. Y. Kukushkin, *Organometallics*, 2017, **36**, 3974-3980; (e) L.-A. Schaper, X. Wei, S. J. Hock, A. Pöthig, K. Öfele, M. Cokoja, W. A. Herrmann and F. E. Kühn, *Organometallics*, 2013, **32**, 3376-3384.

20. D. Huang, P. Zhao and D. Astruc, *Coord. Chem. Rev.*, 2014, **272**, 145-165.

21. (a) D. K. Scrafton, J. E. Taylor, M. F. Mahon, J. S. Fossey and T. D. James, *J. Org. Chem.*, 2008, **73**, 2871-2874; (b) W. Zhai, B. M. Chapin, A. Yoshizawa, H.-C. Wang, S. A. Hodge, T. D. James, E. V. Anslyn and J. S. Fossey, *Org. Chem. Front.*, 2016, **3**, 918-928; (c) W. Zhai, L. Male and J. S. Fossey, *Chem. Commun.*, 2017, **53**, 2218-2221.

22. (a) W. D. Brittain, B. Buckley and J. S. Fossey, *Abstracts of Papers, 250th ACS National Meeting & Exposition, Boston, MA, United States*, 2015, **CATL-207**; (b) W. D. G. Brittain, B. R. Buckley and J. S. Fossey, *Chem. Commun.*, 2015, **51**, 17217-17220; (c) W. D. G. Brittain, B. M. Chapin, W. Zhai, V. M. Lynch, B. R. Buckley, E. V. Anslyn and J. S. Fossey, *Org. Biomol. Chem.*, 2016, **14**, 10778-10782; (d) W. D. G. Brittain, A. G. Dalling, Z. Sun, C. S. Le Duff, L. Male, B. R. Buckley and J. S. Fossey, *ChemRxiv*, 2017, DOI: 10.26434/chemrxiv.5663623.v5663621; (e) W. D. G. Brittain, B. R. Buckley and J. S. Fossey, *ACS Catal.*, 2016, **6**, 3629-3636.

23. (a) J. S. Fossey and T. D. James, in *Reviews in Fluorescence*, eds. C. D. Geddes and J. R. Lakowicz, Springer, 2009, vol. 4, pp. 103-118; (b) J. S. Fossey and T. D. James, in *Supramolecular Chemistry: From Molecules to Nanomaterials*, eds. P. A. Gale and J. W. Steed, John Wiley & Sons Ltd., 2012, vol. 2, ch. 3, pp. 1346-1379; (c) R. Nishiyabu, Y. Kubo, T. D. James and J. S. Fossey, *Chem. Commun.*, 2011, **47**, 1106-1123; (d) R. Nishiyabu, Y. Kubo, T. D. James and J. S. Fossey, *Chem. Commun.*, 2011, **47**, 1124-1150; (e) S. D. Bull, M. G. Davidson, J. M. H. van den Elsen, J. S. Fossey, A. T. A. Jenkins, Y.-B. Jiang, Y. Kubo, F. Marken, K. Sakurai, J. Zhao and T. D. James, *Acc. Chem. Res.*, 2013, **46**, 312-326; (f) W. Zhai, X. Sun, T. D. James and J. S. Fossey, *Chem.-Asian J.*, 2015, **10**, 1836-1848.

24. S. Y. Xu, H. C. Wang, S. E. Flower, J. S. Fossey, Y. B. Jiang and T. D. James, *RSC Adv.*, 2014, **4**, 35238-35241.

25. B. R. Buckley, in *Boron: Sensing, Synthesis and Supramolecular Self-Assembly*, eds. L. Meng, J. S. Fossey and T. D. James, The Royal Society of Chemistry, 2016, pp. 389-409.

26. (a) C. C. C. Johansson Seechurn, M. O. Kitching, T. J. Colacot and V. Snieckus, *Angew. Chem., Int. Ed.*, 2012, **51**, 5062-5085; (b) A. F. Littke and G. C. Fu, *Angew. Chem., Int. Ed.*, 2002, **41**, 4176-4211; (c) N. T. S. Phan, M. Van Der Sluys and C. W. Jones, *Adv. Synth. Catal.*, 2006, **348**, 609-679; (d) S. L. Buchwald, *Adv. Synth. Catal.*, 2004, **346**, 1524-1524; (e) N. Miyaura, *Adv. Synth. Catal.*, 2004, **346**, 1522-1523; (f) R. Martin and S. L. Buchwald, *Acc. Chem. Res.*, 2008, **41**, 1461-1473; (g) S. Ishikawa and K. Manabe, *Chem. Commun.*, 2006, 2589-2591; (h) J. P. G. Rygus and C. M. Crudden, *J. Am. Chem. Soc.*, 2017, **139**, 18124-18137; (i) S. Kozuch and J. M. L. Martin, *ACS Catal.*, 2011, **1**, 246-253; (j) Y. Zhou, X. Zhang, H. Liang, Z. Cao, X. Zhao, Y. He, S. Wang, J. Pang, Z. Zhou, Z. Ke and L. Qiu, *ACS Catal.*, 2014, **4**, 1390-1397.

27. P. S. Kutchukian, J. F. Dropinski, K. D. Dykstra, B. Li, D. A. DiRocco, E. C. Streckfuss, L.-C. Campeau, T. Cernak, P. Vachal, I. W. Davies, S. W. Krska and S. D. Dreher, *Chem. Sci.*, 2016, **7**, 2604-2613.

28. (a) A. F. Littke, C. Y. Dai and G. C. Fu, *J. Am. Chem. Soc.*, 2000, **122**, 4020-4028; (b) T. Hundertmark, A. F. Littke, S. L. Buchwald and G. C. Fu, *Org. Lett.*, 2000, **2**, 1729-1731; (c) A. F. Littke and G. C. Fu, *J. Org. Chem.*, 1999, **64**, 10-11; (d) A. F. Littke and G. C. Fu, *Angew. Chem., Int. Ed.*, 1998, **37**, 3387-3388; (e) G. C. Fu, *Acc. Chem. Res.*, 2008, **41**, 1555-1564.

29. (a) M. Su and S. L. Buchwald, *Angew. Chem., Int. Ed.*, 2012, **51**, 4710-4713; (b) R. A. Altman and S. L. Buchwald, *Nat. Protoc.*, 2007, **2**, 3115-3121.

30. T. E. Barder, S. D. Walker, J. R. Martinelli and S. L. Buchwald, *J. Am. Chem. Soc.*, 2005, **127**, 4685-4696.

31. X. Huang, K. W. Anderson, D. Zim, L. Jiang, A. Klapars and S. L. Buchwald, *J. Am. Chem. Soc.*, 2003, **125**, 6653-6655.

32. (a) N. C. Bruno, M. T. Tudge and S. L. Buchwald, *Chem. Sci.*, 2013, **4**, 916-920; (b) N. C. Bruno, N. Niljianskul and S. L. Buchwald, *J. Org. Chem.*, 2014, **79**, 4161-4166; (c) R. B. Bedford, C. S. J. Cazin and D. Holder, *Coord. Chem. Rev.*, 2004, **248**, 2283-2321.

33. (a) A. Zapf, R. Jackstell, F. Rataboul, T. Riermeier, A. Monsees, C. Fuhrmann, N. Shaikh, U. Dingerdissen and M. Beller, *Chem. Commun.*, 2004, 38-39; (b) WO2004101581A2, 2004.

34. T. E. Pickett, F. X. Roca and C. J. Richards, *J. Org. Chem.*, 2003, **68**, 2592-2599.

35. J. F. Jensen and M. Johannsen, *Org. Lett.*, 2003, **5**, 3025-3028.

36. S.-Y. Liu, M. J. Choi and G. C. Fu, *Chem. Commun.*, 2001, 2408-2409.

37. N. V. Dubrovina, L. Domke, I. A. Shuklov, A. Spannenberg, R. Franke, A. Villinger and A. Börner, *Tetrahedron*, 2013, **69**, 8809-8817.

38. E. M. Schuster, G. Nisnevich, M. Botoshansky and M. Gandelman, *Organometallics*, 2009, **28**, 5025-5031.

39. F. Dolhem, M. J. Johansson, T. Antonsson and N. Kann, *J. Comb. Chem.*, 2007, **9**, 477-486.

40. (a) D. Liu, W. Gao, Q. Dai and X. Zhang, *Org. Lett.*, 2005, **7**, 4907-4910; (b) Q. Dai, W. Gao, D. Liu, L. M. Kapes and X. Zhang, *J. Org. Chem.*, 2006, **71**, 3928-3934; (c) WO2006130842A1, 2006; (d) D. M. Zink, T. Baumann, M. Nieger and S. Bräse, *Eur. J. Org. Chem.*, 2011, **2011**, 1432-1437.

41. B. Choubey, L. Radhakrishna, J. T. Mague and M. S. Balakrishna, *Inorg. Chem.*, 2016, **55**, 8514-8526.

42. H. Oki, I. Oura, T. Nakamura, K. Ogata and S.-i. Fukuzawa, *Tetrahedron Asymmetr.*, 2009, **20**, 2185-2191.

43. J. E. Glover, D. J. Martin, P. G. Plieger and G. J. Rowlands, *Eur. J. Org. Chem.*, 2013, 1671-1675.

44. M. Austeri, M. Enders, M. Nieger and S. Bräse, *Eur. J. Org. Chem.*, 2013, **2013**, 1667-1670.

45. C. Laborde, M.-M. Wei, A. van der Lee, E. Deydier, J.-C. Daran, J.-N. Volle, R. Poli, J.-L. Pirat, E. Manoury and D. Virieux, *Dalton Trans.*, 2015, **44**, 12539-12545.

46. L. Cao, S. Huang, W. Liu and X. Yan, *Organometallics*, 2018.

47. (a) A. H. Christian, Z. L. Niemeyer, M. S. Sigman and F. D. Toste, *ACS Catal.*, 2017, **7**, 3973-3978; (b) M. J. Barrett, G. F. Khan, P. W. Davies and R. S. Grainger, *Chem. Commun.*, 2017, **53**, 5733-5736; (c) M. D. Santos and P. W. Davies, *Chem. Commun.*, 2014, **50**, 6001-6004.

48. C. A. Tolman, *Chem. Rev.*, 1977, **77**, 313-348.

49. H. Clavier and S. P. Nolan, *Chem. Commun.*, 2010, **46**, 841-861.

50. A. Poater, B. Cosenza, A. Correa, S. Giudice, F. Ragone, V. Scarano and L. Cavallo, *Eur J Inorg Chem*, 2009, **2009**, 1759-1766.

51. (a) K. Wu and A. G. Doyle, *Nat Chem*, 2017, **9**, 779-784; (b) Z. L. Niemeyer, A. Milo, D. P. Hickey and M. S. Sigman, *Nature Chem.*, 2016, **8**, 610-617; (c) A. J. Kendall, L. N. Zakharov and D. R. Tyler, *Inorg. Chem.*, 2016, **55**, 3079-3090.

52. F. Lovering, J. Bikker and C. Humblet, *J. Med. Chem.*, 2009, **52**, 6752-6756.

53. I. Colomer, C. J. Empson, P. Craven, Z. Owen, R. G. Doveston, I. Churcher, S. P. Marsden and A. Nelson, *Chem. Commun.*, 2016, **52**, 7209-7212.

54. R. A. Arthurs and C. J. Richards, *Org. Lett.*, 2017, **19**, 702-705.

55. See supporting information for details.

56. See supporting information for details.

57. C. Adamo, C. Amatore, I. Ciofini, A. Jutand and H. Lakmini, *J. Am. Chem. Soc.*, 2006, **128**, 6829-6836.

58. (a) E. Vitaku, D. T. Smith and J. T. Njardarson, *J. Med. Chem.*, 2014, **57**, 10257-10274; (b) R. D. Taylor, M. MacCoss and A. D. G. Lawson, *J. Med. Chem.*, 2014, **57**, 5845-5859; (c) J. Wang and T. Hou, *J. Chem. Inf. Model.*, 2010, **50**, 55-67.

59. The University of Birmingham Scaffold Diversification Resource is a collection of reagents designed to contain functionality commonly found in medicinal chemistry, to allow the late-stage diversification of molecular scaffolds.

60. Should biological activity be observed, and the results deemed of consequence, subsequent future study and resulting reports will be directed towards exploring scope and SAR.

61. L. Chen, P. Ren and B. P. Carrow, *J. Am. Chem. Soc.*, 2016, **138**, 6392-6395.

62. K. Wu and A. G. Doyle, *Nature Chem.*, 2017, **9**, 779.

63. L. Falivene, R. Credendino, A. Poater, A. Petta, L. Serra, R. Oliva, V. Scarano and L. Cavallo, *Organometallics*, 2016, **35**, 2286-2293.

64. D. V. Partyka, T. J. Robilotto, M. Zeller, A. D. Hunter and T. G. Gray, *Organometallics*, 2008, **27**, 28-32.

65. At this stage structural parameters for ligand series 18 have not been determined to a level of satisfactory confidence to permit inclusion in this report. Without XRD data to corroborate any assumptions made in structural minimisations too many uncertainties remain in drawing any conclusions from imposed correlations.

66. (a) J. S. Fossey and W. D. G. Brittain, *Org. Chem. Front.*, 2015, **2**, 101-105; (b) D. T. Payne, J. S. Fossey and R. B. P. Elmes, *Supramol. Chem.*, 2016, **28**, 921-931.